FREE PION ABSORPTION BY LIGHT NUCLEI

A Thesis Submitted
in Partial Fulfilment of the Requirements
for the Degree of

DOCTOR OF PHILOSOPHY

By

N. CHANDRASEKHAR

to the

DEPARTMENT OF PHYSICS

INDIAN INSTITUTE OF TECHNOLOGY, KANPUR

AUGUST, 1981

To HIM

Sweet & Supreme

CERTIFICATE

Certified that the work presented in this thesis is the original work of Mr. N. Chandrasekhar carried out under my supervision.

This work has not been submitted elsewhere for a degree.

August 1981

(Y.R. WAGHMARE)
PROFESSOR OF PHYSICS

Department of Physics
Indian Institute of Technology
Kanpur, India, 208016.

ACKNOWLEDGEMENTS

I am grateful to Prof. Y.R. Waghmare for his guidance and help even otherwise during the course of this work. I am particularly grateful to him for his encouragement and moral support in moments of despair.

I would like to express my thanks to Prof. V.K. Deshpande for some stimulating discussions and helpful comments. My sincere thanks are also due to Dr. S.K. Sharma for his help in some programming difficulties and useful suggestions & interesting discussions.

It is a pleasure to thank my friends Drs. R.S. Bhalerao Saurabh Rindhani and Mohd. Noman for some useful discussions.

I thank my dear friends U.N.L. Mathur and S. Sriram without whose help, the preparation of this manuscript would have been very difficult.

The Financial help rendered by the Council of Scientific and Industrial Research during part of this work is thankfully acknowledged.

Finally thanks are also due to Mr. S.K. Tewari for speedy and very efficient typing. And thanks are also due to Shri Lallu Singh for cyclostyling.

N. Chandrasekhar

CONTENTS

			Page
LIST OF TABLES			vi
LIST OF FIGURES			vii
SYNOPSIS			xii
CHAPTER 1		PION-NUCLEUS REACTIONS -AN INTRODUCTION	1
		REFERENCES	
CHAPTER 2		FOUNDATIONS	
	A	INTRODUCTION	8
	B	PION NUCLEUS OPTICAL POTENTIAL	9
	C	PION NUCLEON INTERACTION VERTEX	17
	D	SHORT RANGE CORRELATIONS IN NUCLEI	19
	E	FREE PION ABSORPTION FOLLOWED BY THE EMISSION OF SINGLE PROTON	22
		REFERENCES	
CHAPTER 3		POSITIVE PION ABSORPTION BY LITHIUM-6 AND CARBON-12	
	A	INTRODUCTION	32
	B	THEORY OF PION ABSORPTION	33
	C	CALCULATIONS	42
	D	RESULTS AND DISCUSSION	44
	E	CONCLUSIONS	84
		REFERENCES	

Page

CHAPTER 4 POSITIVE PION ABSORPTION BY HELIUM-4

A INTRODUCTION 91
B THEORY OF PROTON DISTORTION 92
C THEORY OF PION ABSORPTION 97
D CALCULATIONS 100
E RESULTS AND DISCUSSION 103
REFERENCES

CHAPTER 5 CONCLUSIONS 111

APPENDIX 113

LIST OF TABLES

		Page
Table 1 :	Pion optical potential parameters for Carbon and Lithium	86
Table 2 :	Expansion coefficients $C^{\ell}_{\bar{n}n}$ for Carbon-12 and Lithium-6	87
Table 3 :	Pion optical potential parameters for Helium	101
Table 4 :	Expansion coefficients $C^{\ell}_{\bar{n}n}$ for Helium-4	102
Table 5 :	Comparison of calculated cross-section with experimental data for the reaction $^{3}He(p,\pi^{+})^{4}He$	109

FIG 12 : Angular distribution for the reaction $^{6}Li\ (\pi^{+},p)^{5}Li$. Study of the relative importance of the two terms in the pion-nucleon interaction vertex.
Pion distorted by the Std. Kisslinger form.
Curve A : With both terms present.
Curve B : With only $\bar{\nabla}_{\pi}$ term present.
Curve C : With only $\bar{\nabla}_{N}$ term present (scaled)
The right axis scale is for curve C.

FIG 13 : Angular distribution for the reaction $^{6}Li\ (\pi^{+},p)^{5}Li$ using Standard Kisslinger Potential. Study of the relative importance of the s-wave term and the p-wave term in the Pion-Nucleus optical potential.
Curve A : With both terms included.
Curve B : With only p-wave interaction
Curve C : With only s-wave interaction (scaled).

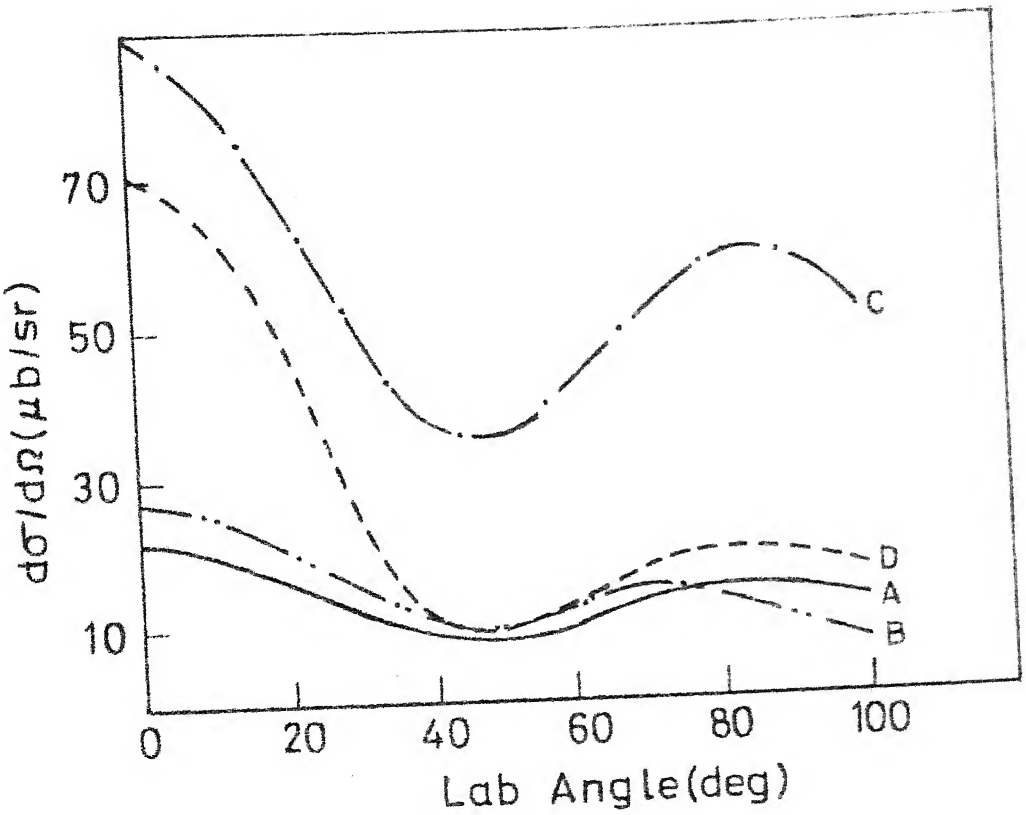
dσ/dΩ(μb/sr)
70
50
30
10
0
20
40
60
80
100
Lab Angle(deg)
C
D
A
B

FIG.14

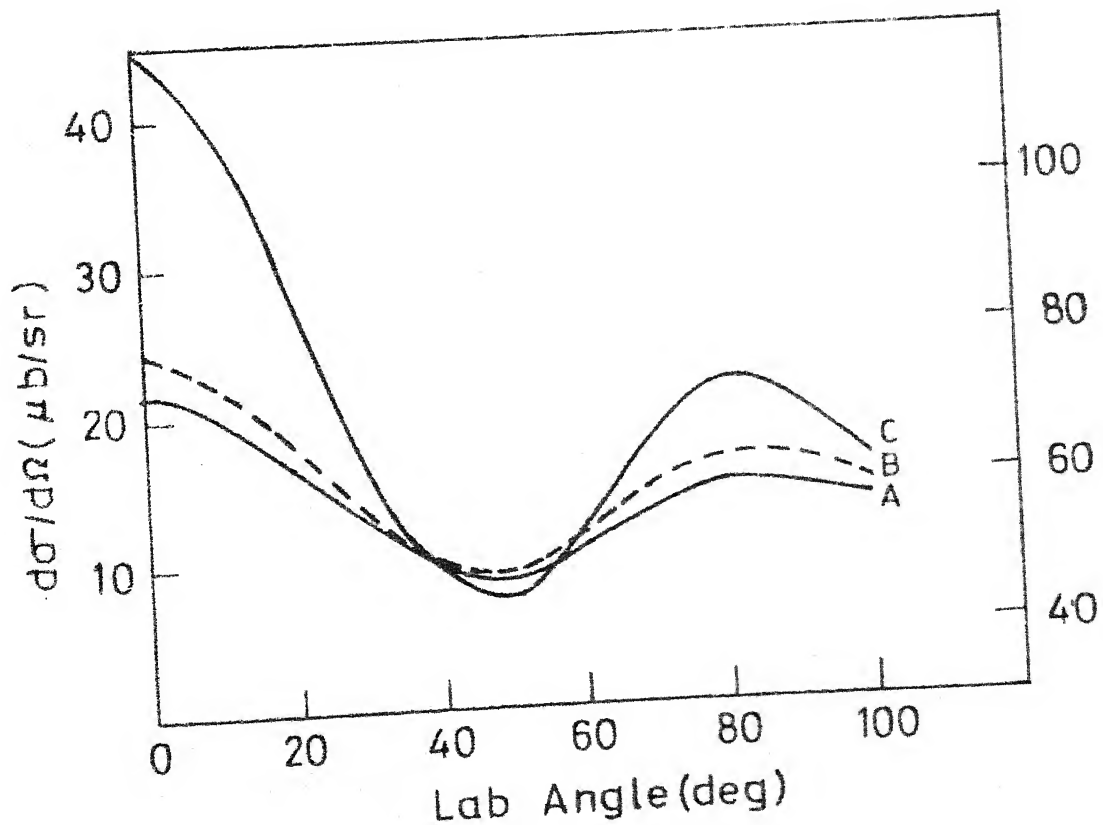
dσ/dΩ(μb/sr)
40
30
20
10
100
80
60
40
0
20
40
60
80
100
Lab Angle(deg)
C
B
A

FIG.15

TABLE OF FIGURES

Page

Fig. 1 : Angular distribution of the crosssection for the reaction $^{12}C(\pi^+,p)^{11}C$ using Standard Kisslinger Potential: Comparison between theoretical (TH) and the best fit (FT) parameter values for b_o and b_1 (Table 1 for values). 47

Fig. 2 : Comparison of angular distribution of crosssection for absorption by $op_{3/2}$ and $os_{1/2}$ neutron. Pion waves distorted by the Standard Kisslinger Potential.

Fig. 3 : Comparison of angular distribution of crosssection for absorption by $op_{3/2}$ and $os_{1/2}$ neutron. Pion waves distorted by the Modified Kisslinger Potential. 50

Fig. 4 : Comparison of angular distribution of crosssection for absorption by $op_{3/2}$ and $os_{1/2}$ neutron. Pion waves distorted by the Local Laplacian Potential.

Fig. 5 : Study of the variation of differential crosssection for the reaction $^{12}C(\pi^+,p)^{11}C$ with proton optical well parameters. Pion waves distorted by the Standard Kisslinger form. Proton optical well parameters in units of Mev: 52

Curve A : $U_o = 9$ $W_o = 15$

Curve B : $U_o = 10$ $W_o = 20$

Curve C : $U_o = 12$ $W_o = 25$

Fig. 6 : Comparison of the differential crosssection for the reaction $^{12}C(\pi^+,p)^{11}C$ with the three kinds of pion distortion

SK : Standard Kisslinger potential
MK : Modified Kisslinger potential
LL : Local Laplacian potential. 54

Fig. 7 : Comparison of the differential crosssection for the reaction $^{12}C(\pi^+,p)^{11}C$ with experimental data.

Curve A : Standard Kisslinger results
Curve B : Modified Kisslinger results
Curve C : Local Laplacian results.
JE : Calculations by Jones and Eisenberg
WK : Calculations by Wienke
EL : Calculations by Leutournex and Eisenberg
RK : Calculations by Rost and Kunz. 57
MP : Calculations by Miller and Phatak.

Fig. 8 : Study of the variation of differential crosssection for the reaction $^{6}Li\ (\pi^+,p)^{5}Li$ with proton optical well parameters. Pion distorted by the Standard Kisslinger Form.
In units of Mev,

Curve A $U_o = 9$, $W_o = 15$
Curve B $U_o = 10$, $W_o = 20$
Curve C $U_o = 12$, $W_o = 25$. 61

Fig. 9 : Study of the variation of differential crosssection for the reaction $^{6}Li(\pi^+,p)^{5}Li$ with proton optical well parameters. Pion distorted by the Modified Kisslinger form.
In units of Mev,

Curve A $U_o = 9$, $W_o = 15$
Curve B $U_o = 10$, $W_o = 20$
Curve C $U_o = 12$, $W_o = 25$.

Fig. 10 : Study of the variation of differential crosssection for the reaction $^{6}Li(\pi^+,p)^{5}Li$ with proton optical well parameters. Pion distorted by the Local Laplacian form.
In unit of Mev,

Curve A $U_o = 9$, $W_o = 15$
Curve B $U_o = 10$, $W_o = 20$
Curve C $U_o = 12$, $W_o = 25$. 63

Fig. 11 : Angular distribution for the reaction $^{6}Li(\pi^+,p)^{5}Li$. Study of relative importance of pion distortation, Nuclear correlations and proton distortion. Pion distorted by the Standard Kisslinger Potential.

Curve A All effects included.
Curve B Pion distortion by strongfield excluded (scaled)
Curve C Nuclear correlations excluded.
Curve D Proton distortion excluded.

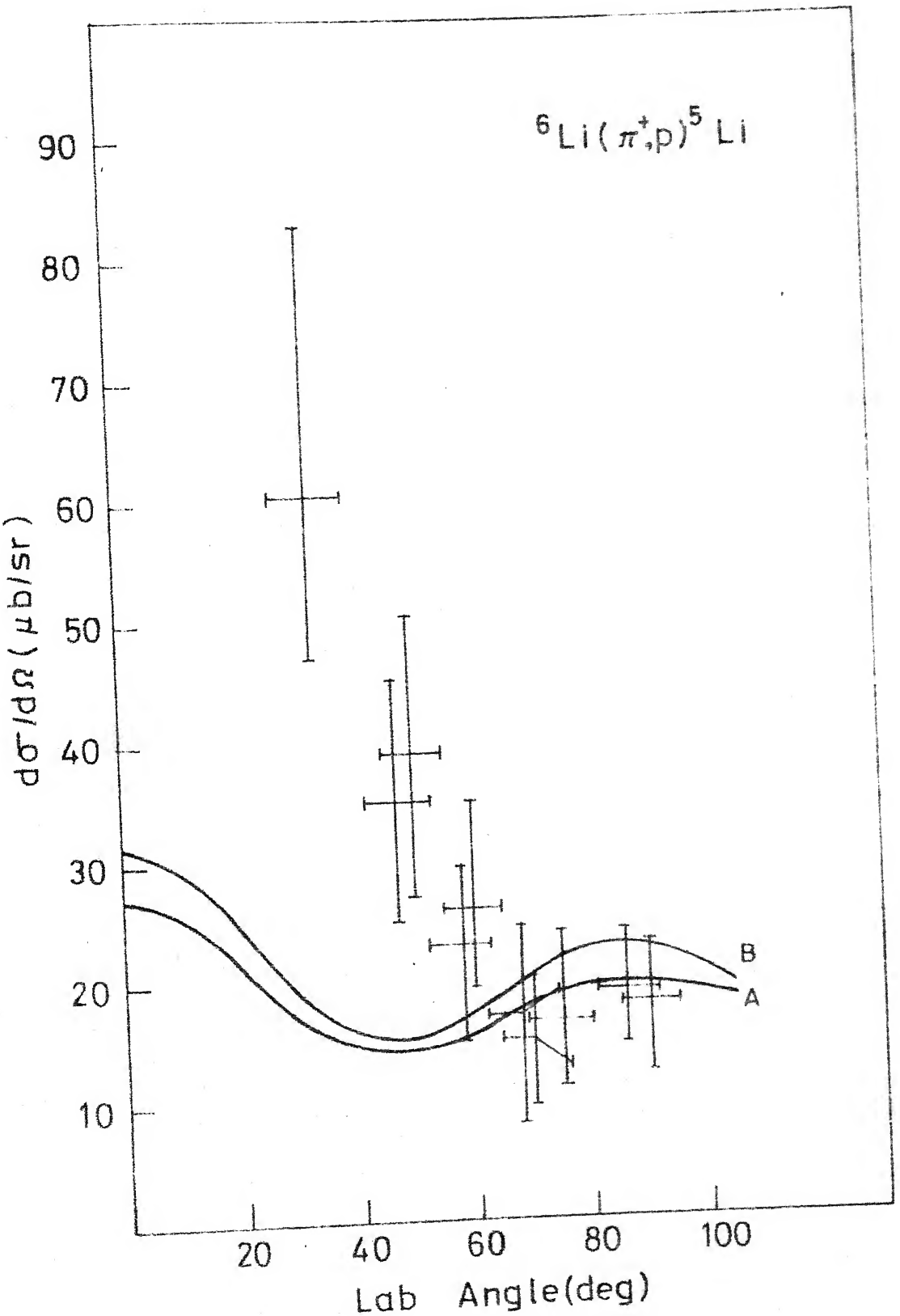
$^6Li(\pi^+,p)^5Li$
90
80
70
60
50
40
30
20
10
$d\sigma/d\Omega$ (μb/sr)
B
A
20
40
60
80
100
Lab Angle(deg)

FIG. 21

Fig. 12 : Angular distribution for the reaction $^{6}Li(\pi^{+},p)^{5}Li$. Study of the relative importance of the two terms in the pion-nucleon interaction vertex. Pion distorted by the Standard Kisslinger form.

Curve A : With both terms present

Curve B : With only $\bar{\nabla}_{\pi}$ term present

Curve C : With only $\bar{\nabla}_{N}$ term present (scaled)

The right axis scale is for curve C. 66

Fig. 13 : Angular distribution for the reaction $^{6}Li(\pi^{+},p)^{5}Li$ using Standard Kisslinger Potential. Study of the relative importance of the S-wave term and the p-wave term in the Pion-Nucleus optical potential.

Curve A : With both terms included
Curve B : With only p-wave interaction
Curve C : With only s-wave interaction (scaled)

Fig. 14 : Angular distribution for the reaction $^{6}Li(\pi^{+},p)^{5}Li$ using Modified Kisslinger Potential. Study of relative importance of pion distortion, Nuclear correlations and proton distortion.

Curve A : All effects included
Curve B : Pion distortion by strongfield excluded (curve scaled)
Curve C : Nuclear correlations excluded
Curve D : Proton distortion excluded. 69

Fig. 15 : Angular distribution for the reaction $^{6}Li(\pi^{+},p)^{5}Li$ using Modified Kisslinger potential. Study of the relative importance of the two terms in the pion-nucleon interaction vertex.

Curve A : With both terms present

Curve B : With only $\bar{\nabla}_{\pi}$ term present

Curve C : With only $\bar{\nabla}_{N}$ term present.

Fig. 16 : Angular distribution for the reaction $^{6}Li(\pi^{+},p)^{5}Li$ using Modified Kisslinger potential. Study of the relative importance of the s-wave term and the p-wave term in the pion nucleus optical potential.

Curve A : With both terms included
Curve B : With only p-wave interaction
Curve C : With only s-wave interaction (scaled). 72

19. G.A. Miller, Nucl. Phys. A223 (1974) 477.

20. E. Kujawski and G.A. Miller, Phys. Rev. C9 (1974) 1205.

21. L.S. Kisslinger and F. Tabakin, Phys. Rev. C9 (1974) 183.

22. R. Mach, Phys. Lett. 40B (1972) 46; Nucl. Phys. A205 (1973) 56.

23. R.J. Glauber in Lectures in Theoretical Physics ed.s. W.E. Britten and L.G. Dunham (Interscience N.Y. 19 Vol. I P. 315.

24. R.J. Glauber in High Energy Physics and Nuclear Structure ed. G. Alexander (John Wiley and Sons N.Y. 1967) P. 311.

25. D.F. Jackson Nuclear Reactions (Metiven and Co. London 1970) P. 64.

26. D.U.L. Yu. Ann. Phys. 38 (1966) 392.

27. Same as Ref. 7.

28. D.M. Brink and G.R. Satchler Angular Momentum (Clarendon, Oxford 1968) P. 52 and Ref. 5.

29. Reference 28, P. 56.

30. Abramowitz M. and I. Stegun in Handbook of Mathematical Functions (Dover Publications, NY) formulas 25.5.10, P. 896.

31. R.A. Eisenstein and G.A. Miller Comp. Phys. Comm. 8 (1974) 130.

32. E.H. Auerbach, D.M. Fleming and M.M. Sternheim, Phys. Rev. 162 (1967) 1683.

33. L.R.B. Elton, Nuclear sizes (Oxford Univ. Press London, 1969).

34. R. Hofstadter, Electron Scattering and nuclear and Nucleon Structure (Benjamin, NY 1963).

35. L.R.B. Elton and A. Swift Nucl. Phys. A 94 (1967) 52.

36. G.M. Perey and F.C. Perey Atomic Data and Nuclear Date Tables 17 (1976) 1.

$$(-\bar{\nabla}^2 + \mu^2)\psi = (E_o^2 - 2V_c E_o + V_c^2 - 2E_o V_N)\psi \qquad (17)$$

The coulomb potential has been calculated assuming the nucleus to be a uniformly charged sphere.

For the pion-nucleus optical potential, we have employed, in turn, the standard Kisslinger form, the Modified Krisslinger form and the Local Laplacian form. Further details are the same as that given in sec. B1, chap. 3.

C2 The Nuclear wavefunction

The absorption of pion is followed by liberation of large amount of energy and a consequent high momentum transfer. This necessitates a correct choice of nuclear wavefunctions which incorporate short range correlations. Hence the wavefunctions has been generated by a HF type variational calculation[1] employing a spherically symmetric HF field for the Helium-4 nucleus. With this prescription, the wavefunction is given by

$$|\text{Nucleus}\rangle = \sum_m \langle jmj{-}m|00\rangle\ \psi^{HF}_{\text{neutron}}(jm)\ \psi^{HF}_c(j{-}m) \qquad (18)$$

$$= \sum_m \frac{(-1)^{j-m}}{\sqrt{2j+1}} \sum_n c^{\ell}_{\bar{n}n} |n\ell jm\rangle_{HO}\ \psi^{HF}_c(j{-}m) \qquad (19)$$

$$= \sum_m \frac{(-1)^{j-m}}{\sqrt{2j+1}} \sum_{n\lambda\Lambda} c^{\ell}_{\bar{n}n} \langle \ell\lambda\tfrac{1}{2}\Lambda|jm\rangle\ |n\ell\lambda\rangle \chi_{\frac{1}{2}\Lambda}\ \psi^{HF}_c(j{-}m) \qquad (20)$$

Fig. 17 : Angular distribution of the crosssection for the reaction $^{6}Li(\pi^{+},p)^{5}Li$ using Local Laplacian potential. Study of relative importance of pion distortion, Nuclear correlations and proton distortion.

Curve A : All effects included
Curve B : Pion distortion by strongfield excluded (curve scaled)
Curve C : Nuclear correlations excluded
Curve D : Proton distortion excluded. 72

Fig. 18 : Angular distribution for the reaction $^{6}Li(\pi^{+},p)^{5}Li$ using Local Laplacian Potential. Study of the relative importance of the two terms in the pion-nucleon interaction vertex.

Curve A : With both terms present
Curve B : With only $\bar{\nabla}_{\pi}$ term present
Curve C : With only $\bar{\nabla}_{N}$ term present (scaled). 75

Fig. 19 : Angular distribution for the reaction $^{6}Li(\pi^{+},p)^{5}Li$ using Local Laplacian Potential. Study of the relative importance of the s-wave term and the p-wave term in the pion-nucleus optical potential.

Curve A : With both terms present
Curve B : With only b_1 term
Curve C : With only b_o term (scaled).

Fig. 20 : Comparison of the differential crosssection for the reaction $^{6}Li\ (\pi^{+},p)^{5}Li$ with the three kinds of pion distortion.

K : Standard Kisslinger potential (scaled)
MK : Modified Kisslinger potential (scaled)
LL : Local Laplacian potential. 77

Fig. 21 : Comparison of the differential crosssection for the reaction $^{6}Li(\pi^{+},p)^{5}Li$ with the experimental data.

Curve A : Results with Modified Kisslinger Potential (scaled)
Curve B : Results with Standard Kisslinger Potential (scaled). 79

Fig. 22 : Comparison of the differential crosssection for the reaction $^{6}Li(\pi^{+},p)^{5}Li$ with experimental data. Smooth curve (—) is the result obtained by employing Local Laplacian potential to distort pion waves. Dashed (----) curve is that obtained by Wienke. 82

Fig. 23 : Differential crosssections for the reaction $^{4}He(\pi^{+},p)^{3}He$.

Curve A : Results obtained with Standard Kisslinger potential
Curve B : Results obtained with Modified Kisslinger potential.
Curve C : is the result of the calculation with protons distorted by a variational calculation and pion plane (scaled). 105

Fig. 24 : Differential crosssection for the reaction $^{4}He(\pi^{+},p)^{4}He$ using Local Laplacian form to distort pion waves (scaled). 107

curves A and B. Further, all the curves A,B and D exhibit a minima around 80^{o}. On the other hand curve C in Fig. 23 is obtained by taking into account the proton distortion through the variational approach however this ignores the incident pion distortion. This result is one order lower than that of curve D. This is expected because curve D takes into account both the coulombic and nuclear distortion of the pion. However curve C does not exhibit any minima. In fact this is consistent with other results which ignore pion distortion[11,12] where the calculations have been done on ^{12}C and ^{16}O.

Unfortunately no experimental results are available on $^{4}He\ (\pi^{+},p)^{3}He$ reaction. However Gabathuler[13] et. al have measured the differential crosssection for the reaction $^{3}He(p,\pi^{+})^{4}He$ (g.s.) for $\theta = 0^{o}$ corresponding to the proton kinetic energy of 600 Mev. The measured crosssection in the lab frame comes out to be $18 \pm 2\ \mu b/sr$. B. Tatischeff[14] et. al have measured the differential crosssection for the reaction $^{3}He\ (p,\pi^{+})^{4}He$ corresponding to the proton kinetic energy at 415 Mev. For $\theta = 0^{o}$, their data indicates a value of around $13\ \mu b/sr$.

Applying the principle of detailed balance[15], the crosssections of the two reactions are related by[16]

SYNOPSIS

FREE PION ABSORPTION BY LIGHT NUCLEI

A thesis submitted in partial fulfilment of the requirements for the degree of DOCTOR OF PHILOSOPHY by Mr. N. Chandrasekhar to the Department of Physics, Indian Institute of Technology, Kanpur-208016.

August 1981

A new era in pion physics was ushered in with the advent of meson factories. It is because the pion possesses a totally different identity from the nucleon giving rise to new possibilities in the investigation of nuclear structure. This is by virtue of the pion being a spin zero boson and available in three charge states π^+, π^o and π^-.

Among the multifarious reactions possible with pion, the study of (π^+,p) reactions are attractive for a variety of experimental and theoretical reasons. The utility of studying this reaction is four-fold.

a) The high momentum transfers involved ($\sim$ 500 Mev/c) provide a method for probing the short range correlations.

b) This reaction can be used to test the perturbation theory approach used in the study of pion absorption phenomena.

c) This reaction may throw light on the mechanism of pion absorption.

d) This can be used to study the single hole states in nuclei.

The earlier calculations have either ignored the nuclear correlations which is expected to be important or have taken into account nuclear correlations, with pion and proton taken to be plane waves.

The present investigation incorporates all the effects such as the initial pion distortion in the presence of coulombic and nuclear field of the absorbing nucleus prior to its absorption, the correlated wavefunctions for the nucleons and the distortion of the emitted proton in the field of the residual nucleus. In this context, one of the ingenious ways devised to tackle the problem of short range correlations is the unitary model operator approach (UMOA). With this, a generalized Hartree-Fock calculation can be carried out, starting with even singular interactions. The resulting wavefunction incorporates partially the short range correlations. One of the ways to put this into test is by means of pion absorption reactions where large momentum transfers are involved.

The thesis consists of five chapters. The first chapter provides a short introduction to the pion-nucleus interactions in general. The second chapter describes a) the background physics involved in the formalism ,

b) gives a brief review of experimental and theoretical work done on this reaction

and c) the motivating factors which prompted us to pursue the present investigation.

Chapter 3 gives details of our work on the positive pion absorption by Carbon and Lithium nuclei. The incident energy of pion is 70 Mev. The first part describes the formalism developed by us to study this reaction and the second part details the results and conclusions. The distortion of the incoming pions is tackled by solving the Klein-Gordon equation employing in turn three kinds of pion-nucleus optical potentials viz the standard Kisslinger form, the Modified Kisslinger form and the Local Laplacian form. This has been done with a view to study their effects upon the crossection, in the presence of nuclear correlations. These are density dependent potentials. For the matter density, the density function generated from our Hartree-Fock wavefunctions has been employed. The coulomb potential has been calculated assuming the nucleus to be a uniformly charged sphere of finite radius. The nuclear wavefunctions employed are generated by a radial Hartree-Fock calculations. The sussex interaction is the basis for this calculations. The resulting wavefunctions incorporates short range correlations. Owing to its high kinetic energy ($\sim$ 160 Mev) the distortion of the proton wave is treated according to high energy (Glauber) approximation

starting from a complex square well potential. The cross-sections have been calculated. The results are in good agreement with the experiment when the pion distortion is accounted through Local Laplacian potential whereas the other two potentials give a higher value for crosssection. Further investigative analysis include the relative importance of pion distortion, nuclear correlations and the proton distortion, the sensitivity of the crossection with respect to certain parameters like the oscillator well parameter α, the proton optical well parameters etc., the ambiguity in the ps-pv interaction vertex employed and the qualitative and quantitative differences in the crosssection when the three kinds of pion distortions are employed in the presence of nuclear correlations. It is found that the undesirable sensitivities found in some previous calculations disappear in the presence of pion distortion and nuclear correlations.

Chapter 4 describes the mechanism of positive pion absorption by Helium-4. This was motivated by two considerations. First is the reasonable success achieved by the present formalism in the case of Carbon and Lithium, and second is that the radial HF formalism developed should work very well with Helium, this being a 'spherical' nucleus. Hence, the calculations have been done on this reaction in the present formalism. Further, to isolate any characteristic features which might have been induced by a complex square well and high energy approximation,

the proton distortion has been taken into account through a different scheme. In this formalism the proton-Helium 3 system is considered as a two cluster problem. This approach is similar to one-channel approximation in Resonating group method as applied to study low energy scattering phenomena. This variational method has been applied to this reaction to see its effectiveness in scattering phenomena of slightly higher energy. Finally, the crosssections obtained are used to calculate the crosssection of $^{3}He(p,\pi^{+})^{4}He$ reaction using the principle of detailed balance. The results calculated compare favourably with the existing experimental results.

Chapter 5 summarises the conclusions of our findings.

CHAPTER 1

PION NUCLEUS REACTIONS

- AN INTRODUCTION

CHAPTER 1

PION-NUCLEUS REACTIONS-AN INTRODUCTION

Pions came to be known in Nuclear Physics even before its actual discovery in 1947[1], with the meson theory of Nuclear forces propounded by Yukawa[2]. Since then the subject of pion interaction with nucleus has been occupying the attention of physicists. Yet it remains a young field. Particularly the last decade has seen many theoretical and experimental investigations, with the advent of meson factories. What is it that makes this subject worthy of so much attention it has received? There are many factors responsible for this.

1. Pion is a pseudo scalar boson with spin zero. This lack of spin makes the theoretical treatment simpler.

2. Pion being a boson can be created and destroyed singly. Hence the production and absorption processes are fundamentally different from the processes involving nucleons alone.

3. Availability in three charged states makes double charge exchange reactions possible. This provides access to otherwise inaccessible states.

4. The incident pion is a distinct particle from the nucleon in the nucleus. Consequently antisymmetrization with respect to the projectile is not required.

5. At low energy the πN interaction is ten times weaker than the NN interaction. This justifies many approximations in theoretical treatment.

6. The pions are the quanta of nuclear forces. Consequently there is a hope that the interactions with real pions will shed some light upon the NN dynamics.

7. Using π^+ and π^- incident beams in scattering experiments interchanges the roles of neutrons and protons in the process. This provides a means to probe the relative proton and neutron distributions.

8. Stopped pion upon absorption by a nucleon liberates a great deal of energy. Consequently the momentum conservation demands the involvement of atleast two nucleons. This provides a method to study the NN correlations, as well as 'hole' states in nuclei.

Having seen various features which make pion an attractive probe in the investigation of nuclear structure, let us look at some of the possible reactions with pions.

A. Single Charge Exchange Reactions

The charge exchange reactions (π^+,π^0) and (π^0,π^-) are sensitive to neutron density distribution while the reverse

reactions are sensitive to proton density distribution. Thus they furnish a method to study the possible difference between charge and mass distribution in nuclei. In this, they are similar to (p,n) and (n,p) reactions.

B. Double Charge Exchange Reactions

The Double Charge exchange reactions $(\pi^{\pm}, \pi^{\mp})$ are something, unlike nucleons, possible with pions by virtue of its isotopic spin being 1. Such kinds of reaction provide access to nuclear isobaric states not possible with nucleon probes and can be used to study these levels. Further if it involves only two nucleons it may possibly enlighten us about NN correlations in nuclei.

C. $(\pi,\pi X)$ Knock out Reactions

Experiments have been done to measure the total cross-section for the reactions $(\pi,\pi N)$ and $(\pi, \pi NN)$ on some light and intermediate nuclei at different pion energies[3]. One interesting result of such measurements by Chivers et. al.[4] at 180 Mev with π^+ and π^- on ^{12}C, ^{14}N and ^{16}O is the following ratio

$$\frac{\sigma(\pi^-, \pi^- n)}{\sigma(\pi^+,\pi^+ n) + \sigma(\pi^+,\pi^o p)} \simeq 1.0 \pm 0.1 .$$

This is interesting because, in the impulse approximation considering only (3,3) resonance this ratio would be 3.

In addition spectroscopic factors can be deduced from the crosssection measurements and compared with shell model estimates.

D. Pionic Atoms

Like muons, negative pions stopped in the target get trapped by the coulomb field of the host nucleus. Normally it gets trapped in a high n level. It cascades down to lower levels emitting Auger electrons and X-rays. The fact that the pions can interact with nucleus through strong interaction as well, affect the levels of pionic atoms in three ways. It causes a level shift, a level width and a reduced intensity of electromagnetic transitions. Their measurements can throw light upon the mechanism of strong interaction between the pion and the nucleus. Pionic atoms have been systematically studied over the whole periodic table[5]. The data have been explained well within the framework of multiple scattering theory[6].

E. Bound Pion Absorption Reaction (π^-, NN)

A negative pion which stops in matter is eventually captured in an atomic orbit and ultimately absorbed by the nucleus. This reaction has been studied for the last three decades since pion beams became available[7]. In this reaction the nucleus receives practically no momentum but an energy of

about 140 Mev corresponding to the pion rest mass. This corresponds to a momentum transfer of roughly 500 Mev/c. The probability of such momenta in the nuclear wavefunction is very small and therefore absorption by a single nucleon is largely suppressed. Hence this absorption is dominated by two nucleon emission. This reaction provides a means to investigate two hole states in nuclei. Further the absorption being done by two nucleons which would have a high relative momentum, one hopes to learn something about short range NN correlations.

The nuclear absorption of negative pion leads to the ejection of two nucleons, in general. In complex nuclei there is a small probability for the absorption to be followed by the emission of a high energy photon. This process is known as Radiative pion absorption. There is evidence that radiative pion absorption leads to the excitation of spin-isospin collective states in nuclei[8]. And such states are known to be of importance in determining muon capture rates[9]. It is this connection which has stimulated lot of interest in this reaction.

F Free Pion Absorption and Production Reactions $(\pi^+,p),(p,\pi^+)$

The study of (π^+,p) and (p,π^+) reactions on complex nuclei are attractive because only two body states are involved. It provides access to single neutron hole or

particle states in analogy with the neutron pick up or stripping reactions. Unique kinematical signature of the outgoing particle has resulted in good experimental data[10] particularly in (p,π^+) reactions. Further because of large momentum transfers involved these reactions can be used to test the structure of short range correlations in nuclei. They can also be used to study the validity of the one-nucleon model (ONM) for π-absorption and production processes. It has also been suggested that these reactions can be used to study the validity of the perturbation theory approach as applied to low energy pion-nucleus interactions.

REFERENCES

1. M. Conversi, E. Pancini and O. Piccioni, Phys. Rev. 71 (1947) 209.

2. H. Yukawa, Proc. Phys. Math. Soc. Japan 17 (1935) 48.

3. D.S. Koltun in Advances in Nuclear Physics ed. M. Baranger and E. Vogt (Plenum Press Ny 1969) p. 135, 136.

4. D. Chivers, J.J. Domingo, E.M. Rimmer, R.C. Witcomb, B.W. Allardyce and N.W. Tanner, Phys. Lett. 26B (1968) 573.

5. G. Backenstoss, Ann. Rev. Nucl. Scien. 20 (1970) 467.

6. M. Ericson and T.E.O. Ericson, Ann. Phys. 36 (1966) 323.

7. Reference 3 page 174-75.

8. J. Delorme and T.E.O. Ericson Phy. Lett. 21 (1966) 98.

D.K. Anderson and J.M. Eisenberg Phys. Lett. 22 (1966) 164.

9. L.L. Foldy and J.D. Walecka Nuovo Cimento 34 (1964) 1026.

10. J. Hufner , Phys. Reports 21 (1975) 1, p 57.

CHAPTER 2

FOUNDATIONS

A. INTRODUCTION

B. PION NUCLEUS OPTICAL POTENTIAL

C. PION NUCLEON INTERACTION VERTEX

D. SHORT RANGE CORRELATIONS IN NUCLEI

E: FREE PION ABSORPTION FOLLOWED BY THE EMISSION OF SINGLE PROTON

- E1 INTRODUCTION
- E2 REVIEW OF THEORETICAL WORK
- E3 REVIEW OF EXPERIMENTAL WORK
- E4 CONCLUSIONS

REFERENCES

CHAPTER 2

FOUNDATIONS

A. INTRODUCTION

The theoretical analysis of elastic scattering of pions by nuclei has been based on three fundamental approaches.

a) Impulse approximation, with multiple scattering correction in some cases.

b) Phenomenological optical models with parameter fits to the data.

c) Optical models derived from multiple scattering theory.

In order to study pion-nucleus interaction, it is essential that one has sufficient knowledge about pion-nucleon interactions. The pion-nucleon interactions have some important characteristic features in comparison with nucleon-nucleon interactions. Unlike nucleon-nucleon crosssection, the pion-nucleon crosssection exhibits a considerable energy variation. At low energies, the nucleon-nucleon crosssections are in barns while the πN cross-sections are in millibarns. The most striking feature of πN crosssection is the presence of (3,3) resonance at $E_\pi \sim 195$ Mev. However at high energies the NN and πN crosssections tend to be equal (~ 30 mb and ~ 40 mb respectively).

These characteristic features of πN interactions are reflected even in π-Nucleus interactions. Firstly, these reactions often show energy variations indicating the effect of πN resonances. Secondly the π-Nuclear interactions at low energies tend to be weak, being amenable to approximation methods like multiple scattering theory. This provides a means to construct an optical potential between pion and nucleus at least in principle.

B. PION-NUCLEUS OPTICAL POTENTIAL

An optical potential is one that describes the scattering of an incident particle by a nucleus by means of an interaction potential which is independent of the coordinates of the individual nucleons and which depends only on the coordinate of the incident particle with respect to the nucleus as a whole. This approach reduces the complex, many body problem of π-nucleus elastic scattering to an effective two body problem in which the nucleus always remains in its ground state.

Derivation of Optical Potential

It is assumed that the pion-nucleus system is described by the Hamiltonian

$$H = T_\pi + H_N + \sum_{i=1}^{A} v_i \qquad (1)$$

$$= H_o + V \qquad (2)$$

where T_π represents the free pion Hamiltonian and H_N is the nuclear Hamiltonian and v_i represents the pion-nucleon interaction. Three body and higher order forces are assumed to be negligible.

The Lippmann-Schwinger integral equation for scattering is given by

$$T = V + VG_oT \tag{3}$$

where the Green's function is

$$G_o = (E - H_o + i\eta)^{-1} \quad \eta \to 0^+ \tag{4}$$

The division of the Hamiltonian into an unperturbed part $H_o = H_N + T_\pi$ and a perturbation $V = \Sigma v_i$ implies that one has some sort of solution to the nuclear Hamiltonian, H_N. And one is prepared to cope up with the complexities arising with its inclusion in the propagator, which has the effect of burying the nuclear dynamics in the heart of the multiple scattering treatment. One permits this with the knowledge that later on under certain conditions the nuclear effects can be approximated as small.

An exact multiple scattering solution[1] of eqn.(3) is

$$T = \sum_i t_i' + \sum_{ij}' t_i' G_o t_j' + \sum_{ijk}' t_i' G_o t_j' G_o t_k' + \ldots \tag{5}$$

The first term in the series corresponds to scattering by one nucleon, the second to scattering by two nucleons and so on.

The notation Σ' means that two successive scatterings by a single nucleon are to be excluded. Such terms are already included in the definition of t-matrix for scattering of pions from bound nucleons,

$$t'_i = v_i + v_i G_o t'_i \tag{6}$$

It is seen that t'_i contains the full nuclear Hamiltonian in G_o. The pion-free nucleon amplitude satisfies a similar equation but with H_N in G_o replaced by a free one nucleon Hamiltonian. Thus t'_i is a complex many body operator while t_i is not.

The elastic scattering amplitude is given by the nuclear ground state expectation value

$$T_c = \langle 0 | T | 0 \rangle \tag{7}$$

which is a function of pion coordinates only. The optical potential U in analogy with eqn. (3) is defined by

$$T_c = U + U G_o T_c \tag{8}$$

Using eqn. 5, it becomes

$$T_c = \sum_i t'_{ic} + \sum'_{ij} (t'_i G_o t'_j)_c + \sum'_{ijk} (t'_i G_o t'_j G_o t'_k)_c + \cdots \tag{9}$$

Thus the problem of pion-nucleus elastic scattering has been reduced formally to solving a one particle problem with the Hamiltonian $T_\pi + U$.

In principle an optical potential exists but it is energy dependent and non-local. It must also be non-Hermitean due to the loss of flux from the elastic channel to other channels. Useful expressions for U are obtained by making approximations.

1. Impulse approximation

This approximation amounts to

$$t_i' = t_i \ . \tag{10}$$

It is reasonable for energies large compared to nuclear binding energies.

2. Coherant approximation

It is assumed here that the nucleus remains in the ground state throughout the scattering process i.e. no excited nuclear intermediate states contribute.

$$\text{i.e.} \quad (t_i G_o t_j G_o t_k)_c = t_{i_c} G_o \, t_{j_c} G_o \, t_{k_c} \tag{11}$$

consequently eqn. (9) becomes

$$T_c = \sum_i t_{i_c} + \sum'_{ij} t_{i_c} G_o t_{j_c} + \sum'_{ijk} t_{i_c} G_o t_{j_c} G_o t_{k_c} + \ldots \tag{12}$$

3. Large nucleus approximation

If A is large, then one can set $\Sigma' = \Sigma$

Eqn. 12 reads then

$$T_c = \sum_i t_{i_c} + \sum_{ij} t_{i_c} G_o t_{j_c} + \sum_{ijk} t_{i_c} G_o t_{j_c} G_o t_{k_c} + \ldots \tag{13}$$

i.e.

$$T_c = (\Sigma\ t_{i_c}) + (\Sigma\ t_{i_c})\ G_o T_c \tag{14}$$

comparing with (8) one finds

$$U = \sum_i t_{i_c} \tag{15}$$

This is the lowest order optical potential.

4. Static Approximation

The assumption here is that the position of a massive nucleon is unchangeable by the scattering of a pion. Then eqn. (15) becomes

$$\langle \vec{p}' | U | \vec{p} \rangle = \sum_i \langle \vec{p}' | t_i | \vec{p} \rangle\ \rho(\vec{p}' - \vec{p}) \tag{16}$$

where $\vec{p}'$ and $\vec{p}$ are the pion momenta. Here

$$\rho(\vec{q}) = \int e^{i\vec{q}\cdot\vec{r}}\ \rho(\vec{r})\ d^3r \tag{17}$$

is the nuclear form factor, which is the fourier transform of the nuclear density function, which is normalized to unity

$$\int \rho(\vec{r})\ d^3r = 1. \tag{18}$$

A relatively simple optical potential[2] is obtained from eq. (16) if one assumes forward scattering approximation for t.

$$\langle \vec{p}' | t | \vec{p} \rangle\ \rho(\vec{p}' - \vec{p}) \approx \langle \vec{p} | t | \vec{p} \rangle\ \rho(\vec{p}' - \vec{p}) \approx \langle \vec{p}_o | t | \vec{p}_o \rangle\ \rho(\vec{p}' - \vec{p}) \tag{19}$$

Here one assumes first that $\rho(\vec{q})$ drops off rapidly with

increasing q, and then the wavefunction in momentum space is strongly peaked about the incident momentum $\vec{p}_o$. In coordinate space U is now local.

$$U(\vec{r}) = (2\pi)^3 \, A \, \langle \vec{p}_o | t | \vec{p}_o \rangle \, \rho(\vec{r}) \tag{20}$$

where $\langle \vec{p}_o | t | \vec{p}_o \rangle$ is suitably averaged over π-p and π-n amplitudes. Calculations based on this simple model invariably fit, only small angle data. This model fails to take into account, the dominant p-wave character of low energy π-nucleon scattering. Noting that usually $t_\ell \sim p^{2\ell}$ holds Kisslinger[3] substituted into eqn. (16)

$$\begin{aligned} \langle \vec{p}' | t | \vec{p} \rangle &= a_o + a_1 p^2 \cos\theta \\ &= a_o + a_1 \vec{p}' \cdot \vec{p} \end{aligned} \tag{21}$$

obtaining

$$\langle r | U\psi \rangle = (2\pi)^3 \, A \left[a_o \rho \psi - a_1 \, \bar{\nabla} \cdot (\rho \, \bar{\nabla} \, \psi) \right] \tag{22}$$

or in terms of momentum operators

$$U(\vec{r}) = (2\pi)^3 \, A \left[a_o \rho - a_1 \vec{p} \cdot \rho \, \vec{p} \right] \tag{23}$$

Eqn. (22) is the ''standard Kisslinger potential''. This is a density dependent non-local potential. The $\bar{\nabla}\rho$ term suggests a strong surface sensitivity for pion scattering. From eqn. (22) one gets

$$2E_o U\psi = -Ab_o p_o^2 \rho\psi + Ab_1 \, \bar{\nabla} \cdot (\rho \, \bar{\nabla} \, \psi) \tag{24}$$

where

$$b_o = -2(2\pi)^3 E_o a_o / p_o^2 \qquad (25)$$

$$b_1 = -2(2\pi)^3 E_o a_1 \qquad (25)$$

a form suitable for Klein-Gordon equation. The b's are proportional to π-nucleon amplitudes and are independent of nuclear parameters (Here E_o is the total pion energy). They are related to phaseshifts in π-nucleon centre of mass system through[4]

$$b_o = \frac{4\pi}{p^3} \frac{\mu^2+M^2+2E_oM}{M^2} \left[N(\alpha_3+2\alpha_1)/3 + Z\,\alpha_3 \right] A^{-1} \qquad (26)$$

$$b_1 = \frac{4\pi}{p^3} \frac{\mu^2+M^2+2E_oM}{M^2} \left[N(2\alpha_{33}+\alpha_{31}+4\alpha_{13}+2\alpha_{11})/3 + Z(2\alpha_{33}+\alpha_{31}) \right] A^{-1} \qquad (27)$$

where μ is the pion mass, M the nucleon mass and Z,N are proton and neutron numbers. $\alpha_i = \exp(i\delta_i) \sin\delta_i$ where δ_i are the π-nucleon phaseshifts and $i=(2T,2J)$. For a π^- and nucleus (ZN), the factors Z and N are interchanged.

The behaviour of b's have been studied by Auerbach et.al.[4] Since b_1 is dominated by $\alpha_{33}/p^3 \approx (\delta_{33} + i\delta_{33}^2)/p^3$ and δ_{33} has the expected p^3 behaviour, Re b_1 is almost constant for $T_\pi \leq 130$ Mev. And Im b_1 is rapidly increasing with T_π. Im $b_o \sim (2\delta_3^2 + \delta_1^2)/p^2$ has the expected 1/p behaviour. The leading terms in $2\delta_3$ and δ_1, linear in p nearly cancel so that Re $b_o \sim (2\delta_3+\delta_1)/p^2$ is surprisingly constant. It is

clear that the largest uncertainty is associated with Re b_o since moderate deviations from the free π-nucleon amplitudes may spoil the accidental cancellations and lead thereby to much larger values with a $1/p^2$ variation.

Local Laplacian Potential

The Kisslinger model assumes an off-shell pion-nucleon scattering matrix defined by eqn. (21). Other models of off-shell behaviour are also possible. For example one can choose the off-shell pion-nucleon scattering matrix to be a function of the momentum transfer ($\vec{q} = \vec{p}' - \vec{p}$) alone[5]. On shell ($|\vec{p}| = |\vec{p}'| = p_o$) we have

$$\vec{p}' \cdot \vec{p} = (p^2 + \vec{p}'^2)/2 - q^2/2 \qquad (28)$$

$$= p_o^2 - q^2/2 \qquad (29)$$

Thus one can choose alternately the off-shell scattering matrix as

$$\langle \vec{p}' | t | \vec{p} \rangle = a_o + a_1 (p_o^2 - q^2/2) \qquad (30)$$

in the place of eqn. 21.

This results in the Local Laplacian form of the optical potential, which in coordinate space reads

$$U(\vec{r}) = (2\pi)^3 A \left[(a_o + a_1 p_o^2)\rho + \frac{1}{2} a_1 \vec{\nabla}^2 \rho \right] \qquad (31)$$

Modified Kisslinger Potential

Doubts have been expressed about the validity of some of the approximations made in deriving the Standard

Kisslinger form[6]. Rejecting the static approximation, Mach[7] has taken into account the fermi motion of the target nucleons.

This introduces additional terms into Kisslinger potential. The resulting form is

$$U(\vec{r}) = (2\pi)^3 A \left[a_o \rho - a_1 \bar{\nabla}.(\rho \bar{\nabla}) + \frac{E_o}{2M} a_1 \bar{\nabla}^2 \rho \right] \quad (32)$$

C. PION NUCLEON INTERACTION VERTEX

It would be useful to have a hamiltonian formalism to describe pion nucleon interactions. This will be convenient for processes like pion absorption and for kinematical situations in π-nucleus interactions which do not correspond to the kinematics of free π-N scattering. There is no satisfactory theoretical basis for finding such interactions, although in analogy with electrodynamics, field theoretic models have been developed. Particularly the process of pion absorption $\pi + N \rightarrow N$ can take place only 'virtually', that is in the presence of other particles to conserve energy and momentum.

One can start from Lagrangian densities[8]

$$\mathcal{L}_{int} = -i f_{PP} \bar{\psi}_N \gamma_5 \psi_N \phi \quad (33)$$

or

$$\mathcal{L}_{int} = - \frac{i f_{PA}}{\mu} \bar{\psi}_N \gamma_5 \gamma_\nu \psi_N \partial_\nu \phi \quad (34)$$

where interaction (33) is called ps-ps (ps: pseudoscalar) interaction and (34) is ps-pv (pv: pseudovector) interaction.

ϕ is the pionic field and ψ's are the source spinors. A non-relativistic reduction of either terms coupled with the fact that in the non-relativistic limit $\frac{\partial \mathcal{L}_{int}}{\partial \dot{\phi}} \sim \langle \gamma_5 \gamma_4 \rangle$ is small yields the following Hamiltonian

$$H_{int} = f/\mu \; \rho(|\vec{r}-\vec{r}'|) \; \vec{\sigma}.\vec{\nabla}_\pi \; \phi(\vec{r}') \qquad (35)$$

Incorporating isospin invariance this modifies into[8]

$$H_{int} = f/\mu \; \rho(|\vec{r}-\vec{r}'|) \; \vec{\sigma}.\vec{\nabla}_\pi (\vec{\tau}.\vec{\phi}) \qquad (36)$$

For a point nucleon this reduces to

$$H_{int} = f/\mu \; \vec{\sigma}.\vec{\nabla}_\pi \; \vec{\tau}.\vec{\phi} \; \; \delta(\vec{r}-\vec{r}') \qquad (37)$$

This is the Hamiltonian in the static limit. However this does not satisfy Galilean invariance. This invariance can not be strictly defined for virtual particles. In attempts[9], not completely justified, to recover some sort of Galilean invariance, one defines the pion velocity as $\vec{v}_\pi \simeq \vec{k}/\epsilon_k$ and $(\vec{p}+\vec{k}/2)/M = \vec{v}_N$ as the nucleon velocity averaged over momenta before and after absorption. Then $H_o \alpha \; \vec{v}_\pi - \vec{v}_N$ is Galilean invariant in the sense given. Consequently in the non-static limit eq. (37) becomes

$$H_{int} = \left[f/\mu \; (1- \tfrac{\mu}{2M}) \; \vec{\sigma}.\vec{\nabla}_\pi \; \vec{\tau}.\vec{\phi} - \mu/M \vec{\tau}.\vec{\phi} \; \vec{\sigma}.\vec{\nabla}_N \right] \delta(\vec{r}-\vec{r}') \qquad (38)$$

The interaction vertex in the static limit also appears in Chew-Low theory[10]. Barnhill[11] has pointed out that a

careful non-relativistic reduction leads to ambiguity in the coefficient of the second term i.e. in the coefficient λ when eq.(38) is written in the form[12]

$$H_{int} = \left[f/\mu \left(1 - \frac{\lambda\mu}{2M}\right) \vec{\sigma}.\vec{\nabla}_\pi \; \vec{\tau}.\vec{\phi} - \frac{\lambda\mu}{M}(\vec{\tau}.\vec{\phi}) \; \vec{\sigma}.\vec{\nabla}_N \right] \delta(\vec{r}-\vec{r}') \tag{39}$$

This ambiguity has been studied by various authors[13]. In conclusion two main criticisms of non-relativistic model has been levied. Firstly the non-relativistic treatment of a typically relativistic pseudoscalar πN interaction operator is certainly not adequate for all kinematical situations. Secondly it is probably questionable to treat wavefunctions of bound nucleons in a purely non-relativistic fashion especially in such processes involving high momentum components.

D. SHORT RANGE CORRELATIONS IN NUCLEI

Most of the realistic nucleon-nucleon potentials which fit the two body scattering data contain a repulsive core. Such a repulsive core will give rise to strong short range correlations which are not described well by an independent particle model. In the framework of Brueckner's theory, the short range correlations are handled by using the separation method of Mozkowiski and Scott[14] or the reference spectrum method of Bethe, Brando and Petschek[15].

In the separation method[14], the actual NN interaction is decomposed into a short range part v_s and a long range part v_ℓ . The separation distance d is a parameter so chosen as to have the hard core repulsive effects exactly balanced for the low momentum states by enough attraction from the potential outside the core. The remaining potential is then weak and non-singular and hence amenable to treatment by simple perturbation theory.

Another method proposed by Jastrow[16] involves the multiplication of two nucleon wavefunction in shell model basis by two body functions $f(r_{ij})$ which introduce short range correlations. The form of f is such that

$$f(r_{ij}) \to 1 \quad \text{as} \quad r_{ij} \to \infty$$
$$\text{and} \qquad f(r_{ij}) = 0 \text{ for } r_{ij} \leq r_c. \tag{40}$$

This total wavefunction is then used as a trial wavefunction in variational calculation.

Deshalit and Weisskopf[17] goes one step further to introduce a two particle correlation factor $f_{\alpha\beta}(r_{ij})$, which are dependent on $(\alpha\beta)$ unlike the Jastrow correlation factor.

Unitary Model Operator Approach.

In this approach[18] actual nuclear wavefunctions are generated from a set of uncorrelated basis states by a

unitary transformation. The corresponding unitary operator is taken to be of the form exp (iS). The form of S is so chosen that exp(iS) introduces short range correlations in the basis states ϕ. The application of this leads to an effective Hamiltonian

$$H_{eff} = \sum_{n_1 n_2} \langle n_1 | T | n_2 \rangle a^+_{n_1} a^+_{n_2} + \frac{1}{2} \sum_{\substack{n_1 n_2 \\ n_3 n_4}} a^+_{n_1} a^+_{n_2} \langle n_1 n_2 | e^{-iS}$$

$$(T_1+T_2+U_1+U_2+v_{12})\, e^{iS} - (T_1+T_2+U_1+U_2) | n_3 n_4 \rangle a_{n_4} a_{n_3} \quad (41)$$

The higher order terms have been neglected because they are small. The form of U is taken to be harmonic oscillator type to simplify the calculation.

Application of e^{iS} results in

$$e^{iS} \phi_{n_1 n_2} = \psi_{n_1 n_2} \quad (42)$$

where ϕ's are the uncorrelated basis and ψ's are the correlated wavefunctions. The potential v_{12} is split into v^{ℓ}_{12} and v^{s}_{12} such that v^{s}_{12} does not produce any energy shift in the pair state energy. Then

$$H_{eff} = \sum_{n_1 n_2} \langle n_1 | T | n_2 \rangle\, a^+_{n_1} a^+_{n_2} + \sum_{\substack{n_1 n_2 \\ n_3 n_4}} a^+_{n_1} a^+_{n_2} a_{n_4} a_{n_3}$$

$$\langle \psi_{n_1 n_2} | v^{\ell}_{12} | \psi_{n_3 n_4} \rangle. \quad (43)$$

Having thus converted the realistic Hamiltonian containing hard core into an effective one which is regular, one can, set up and solve Hartree-Fock equation. The wavefunction employed in the present work are the results of one such calculation[19] where spherical HF field was assumed and a radial Hartree-Fock calculation was performed.

E FREE PION ABSORPTION FOLLOWED BY THE EMISSION OF SINGLE PROTON

E1 INTRODUCTION

The present work addresses itself to the study of free pion absorption by light nuclei with the emission of a single proton i.e.

$$\pi^+ + {}^{Z}A \rightarrow p + {}^{Z}A\text{-}1$$

The interest in this reaction is prompted by its utility value.

This reaction is similar to the (p,2p) or (e, e'p) reactions[20] used to study single hole states in nuclei. But the latter reactions suffer from the disadvantage of the need to detect two particles in the final state. On the contrary this reaction involves a single particle with unique kinematical signature.

The reaction involves only two bodies either in the initial state or in the final state. This lends itself to relatively straightforward treatment from both experimental

and theoretical points of view. Consequently this reaction can be used to study the perturbation theory approach used in bound pion absorption reactions[21] or radiative pion capture[22]. Even though alternative methods exist for handling the pion-nucleus interactions, the standard[23] non-relativistic limit of the pseudo scalar-pseudo vector interaction is usually the simplest means to introduce a detailed treatment of nuclear structure. Then it is essential to ascertain the validity of perturbation theory approach. One cannot use the two nucleon emission process following a bound pion absorption as there are three bodies in the final state. This makes it difficult to isolate the possible discrepancies arising from perturbation theory approach. One cannot equally rely upon the radiative absorption of pions. Here the presence of electromagnetic field leads to the dominance of the so called gauge invariance term[24]. This term involves a point interaction between the pion, nucleon and the photon and hence does not yield information on the use of perturbation theory for the usual pion-nucleon vertex. Furthermore it is more suitable than the process of single nucleon emission following bound pion absorption, for the latter suffers from the need to detect a neutron in the final state and from an even greater degree of energy-momentum forbiddenness.

E2 REVIEW OF THEORETICAL WORK

The first calculation of this reaction was done by Letournex and Eisenberg[25] in the formalism of first order perturbation theory. In this calculation the incident pion and the outgoing proton were taken to be plane waves whereas the neutron was represented by HO wavefunction. The cross-section thus calculated has several undesirable features. First of all, the crosssection is extremely sensitive to the oscillator well parameter α changing by a factor of eight to three orders for different angles as one varies α over allowable range. It is also sensitive to the proton momentum and ambiguities in the interaction vertex. The calculated crosssection matches well with the data points corresponding to 20^{o} and 32^{o} in the case of ^{12}C as measured by Amato et. al.[32] In view of the fact that the formalism has ignored important effects like pion distortion, nuclear correlations and the proton distortion and is extremely sensitive to parameters like α, one can say that this agreement with experiment is only fortuitous.

Jones and Eisenberg[26] have employed distorted waves for both pion and proton in their calculation, while the neutron wavefunction is generated using a Wood-Saxon well. The pion waves are generated using both Kisslinger and Kroll-Kisslinger potentials. Kroll-Kisslinger potential is a modification of

Kisslinger potential incorporating Lorentz-Lorentz effect. The pion distortion is found to stabilise the crosssections, unlike the previous calculation. However the calculated crosssection is much higher than the experimental value. Further the Kroll-modification does not seem to affect the (π^+,p) crosssection. In fact even in bound pion studies, Ericson's work[34] fails to confirm definitely the presence of a Lorentz-Lorentz type dependence in the average nuclear potential as seen by pions. Kaushal and Waghmare[27] have employed HF wavefunctions for the neutron, to take into account nuclear correlations. The pion and proton are taken to be plane. Their calculation establishes the importance of nuclear correlated wavefunction in view of high momentum transfers involved in the process. The crosssection is found to increase by one order with the inclusion of correlations. However in view of the plane waves, the crosssection is once again sensitive to α. Rost and Kunz[28] have studied the (π^+,p) reaction assuming single neutron pickup in a distorted wave Born approximation framework. Pion distortion is accounted through Kroll-Kisslinger model. However the π-N coupling constant f was used as an adjustable parameter to normalise the calculated results with experimental data. Their success is only qualitative.

A field theoretical method was employed by Wienke[29] to calculate the crosssection for this reaction. The pion and

proton were taken to be plane while Harmonic oscillator wavefunction represented the neutron. However pion re-scattering was taken into account. The inclusion of rescattering terms stabilised the crosssection w.r.t. variation in α.

Miller and Phatak[30] studies this reaction assuming a pickup mechanism in a DWBA framework. The Kisslinger and Local Laplacian potential exhibit a divergent off-shell behaviour. Employing a different off-shell extrapolation with non-divergent behaviour, the pion waves were generated. Only the static part of the non-relativistic interaction vertex was employed. The calculated crosssection seems to agree with the older data of Witten et. al.[31].

E3 REVIEW OF EXPERIMENTAL WORK

The first experimental measurements were done by Witten et. al.[31]. They measured the differential crosssection for carbon at $\theta = 0^{\circ}$ and 11° for pion kinetic energy of 73 Mev and 68 Mev respectively. The resolution was 14 Mev (FWHM). The crosssections were obtained for capture by $op_{3/2}$ neutron leading to ground state and low lying excited states upto 5 Mev.

The next experimental measurement by Amato et. al.[32] studied this reaction on ^{6}Li, ^{9}Be, ^{12}C and ^{16}O corresponding to pion kinetic energy of 70 Mev. The experimental resolution

was 3 Mev (FWHM). In the case of ^{12}C, the differential crosssections at $\theta = 20^{o}$ and $\theta = 32^{o}$ were measured leading to ground state and excited states upto 8 Mev. However in the case of Lithium, systematic measurement have been done for a number of angles in the range $\theta = 33^{o}$ to $\theta = 90^{o}$ leading to ground state and the broad unbound $p_{1/2}$ state of ^{5}Li which occurs at approximately 4 Mev. In the case of ^{9}Be and ^{16}O only upper limits of the differential crosssection at $\theta = 25^{o}$ have been obtained.

The latest measurement by Bachelier et. al.[33] studies the oxygen system. The differential crosssections have been systematically measured for θ lying between 0^{o} and 120^{o}, leading to the $(p_{3/2})^{-1}$ hole state at 6.18 Mev and the $(p_{1/2})^{-1}$ hold ground state of ^{15}O. Measurements have been done corresponding to a pion kinetic energy of 66 Mev. The impressive feature of this measurement is the separation of the crosssection w.r.t. these two levels. The energy resolution is 3.2 Mev (FWHM).

E4 CONCLUSIONS

Summing up the work that has been done so far, it is found that one is still not competent enough to comment about the perturbation theory approach in view of the various approximation which go into the process. It is because, inclusion of pion distortion consistently give higher values

for crosssection. Further the work of Kaushal et. al.[27] has established the importance of correlated wavefunctions for neutron. This is obvious from the kind of momentum transfers involved in the process. Hence it is essential that one includes all the effects like pion distortion, nuclear correlations and proton distortion. And it is interesting to see then, the sensitivity of the crosssection with α, the ambiguity in the interaction vertex etc. In view of the importance of off-shell effects in pion reactions, it is also essential to study the pion distortion through different kinds of optical potentials developed with different off-shell extrapolations. As for rescattering effects, the use of pion-nucleus optical potential in a formalism incorporating rescattering would amount to double counting.

REFERENCES

1. K.M. Watson, Phys. Rev. 89 (1953) 571, ibid, Phys. Rev. 105 (1957) 1388.

2. W.F. Baker, J. Rainwater and R.E. Williams, Phys. Rev. 112 (1958) 1763, ibid, Phys. Rev. 112 (1958) 1773.

3. L.S. Kisslinger, Phys. Rev. 98 (1955) 761.

4. E.H. Auerbach, D.M. Fleming and M.M. Sternheim, Phys. Rev. 162 (1967) 1683.

5. H.K. Lee and H. McManus, Nucl. Phys. A167 (1971) 257.

   G. Faldt, Phys. Rev. C5 (1972) 400.

   J.H. Koch and M. Sternheim, Phys. Rev. C6 (1972) 1118.

6. E. Leader, Nucl. Phys. 26 (1961) 177.

   C. Schmit, Orsay preprint IPNO/TH71-37 (1971)(quoted in Ref. 7).

7. R. Mach, Phys. Lett. 40B (1972) 46; ibid Nucl. Phys. A205 (1973) 56.

   E. Kujawski and G.A. Miller, Phys. Rev. C9 (1974) 1205.

   L.S. Kisslinger and F. Tabakin, Phys. Rev. C9 (1974) 188.

8. H. Muirhead in The Physics of Elementary Particles (Pergamon. N.Y. 1965) p. 355, 385.

9. L.L. Foldy Phys. Rev. 84 (1951) 168.

10. G. Chew and F. Low, Phys. Rev. 101 (1966) 1570.

11. M.V. Barnhill, Nuc. Phys. A131 (1969) 106.

12. G.A. Miller, Nucl. Phys. A223 (1974) 477.

13. I.T. Cheon, Prog. Theor. Phys. Suppl. (1968).

    J.L. Friar, Phys. Rev. C10 (1974) 955.

    M. Bolsterli, W.R. Gibbs, B.F. Gibson and G.J. Stephenson, Phys. Rev. C10 (1974) 1225.

    J.M. Eisenberg, J.V. Noble and H.J. Weber, Phys. Rev. C11 (1975) 1048.

14. S.A. Moskowski and B.L. Scott, Ann. Phys. (N.Y.) 11 (1960) 65.

15. H.A. Bethe, B.H. Brandow and A.G. Petschek, Phys. Rev. 129 (1963) 225.

16. R.J. Jastrow, Phys. Rev. 38 (1955) 1479.

17. A. DeShalit and V.F. Weisskopf, Ann-Phys.,(NY) 5 (1958) 282.

18. F. Villars in Proceedings of the International School of Physics "E. Fermi", Course 23 1961 (Academic, N.Y. 1963) p. 1.

J. Da. Providencia and C.M. Shakin, Ann. Phys. (NY) 30 (1964) 95; Nucl. Phys. 65 (1965) 54 and 75

C.M. Shakin, Y.R. Waghmare and M.H. Hull, Phys. Rev. 161 (1967) 1006.

C.M. Shakin, Y.R. Waghmare, M.H. Hull and M. Tomaselli, Phys. Rev. 161 (1967) 1015.

19. I. Kakkar, Nuclear Structure Studies in Hartree-Fock Representation Ph.D. Thesis, 1969, IIT Kanpur (unpublished).

20. G. Jacob and Th. A.J. Maris, Revs. Mod. Phys. 38 (1966) 21.

21. P. Huguenin, Z. Phys. 167 (1962) 416.

R.I. Jibuti and T.I. Kopaleishvili, Nucl. Phys. 55 (1964) 337.

J. Letournex, Nucl. Phys. 81 (1966) 665.

R.S. Bhalerao and Y.R. Waghmare, Nucl. Phys. A298 (1978) 367 and references therein.

22. D.K. Anderson and J.M. Eisenberg, Proc. Williamsburg Conf. on intermediate energy physics (1966).

23. S.S. Scheweber in An Introduction to quantum field theory (Row, Peterson and Evanston, Ill., 1961) p 301, 373.

24. Reference 22

25. J. Letournex and J.M. Eisenberg, Nucl. Phys. 87 (1966) 331.

26. W.B. Jones and J.M. Eisenberg, Nucl. Phys. A154 (1970) 49.

27. R.S. Kaushal and Y.R. Waghmare, Phys. Lett. B31 (1970) 637.

28. E. Rost and P.D. Kunz, Phys. Lett. B43 (1973) 17.

29. B.R. Wienke, Prog. Theor. Phys. 49 (1973) 1220.

30. G.A. Miller and S.C. Pathak, Phys. Lett. B51 (1974) 129.

31. T.R. Witten, M. Blecher and K. Gotow, Phys. Rev. 174 (1968) 1166.

K. Gotow in High Energy Physics and Nuclear Structure III 1969, ed. S. Devons (Plenum, NY, 1970) p 374.

32. J. Amato, R.L. Burman, R. Macek, J. Oostens,

W. Shlaer, E. Arthur, S. Sobottka and W.C. Lam,Phys. Rev. C9 (1974) 501.

33. D. Bochelier, J.L. Boyard, T. Hennino, J.C. Jourdain

P. Radvanyi and M. Roy-Stephan, Phys. Rev. C15 (1977) 2139.

34. M. Ericson and T. Ericson, Ann. of Phys. 3b (1966) 323

T. Ericson in Interaction of high energy particles with nuclei, Proc. of Int. School of Physics Enrico Fermi Course XXXVIII (Academic, NY, 1967) p 253.

CHAPTER 3

POSITIVE PION ABSORPTION BY LITHIUM-6 AND CARBON-12

A. INTRODUCTION

B. THEORY OF PION ABSORPTION

C. CALCULATIONS

D. RESULTS AND DISCUSSION

E. CONCLUSIONS

REFERENCES

CHAPTER 3

POSITIVE PION ABSORPTION BY LITHIUM-6 AND CARBON-12

A : INTRODUCTION

The Pion as a nuclear probe and its utility in understanding nuclear structure has become increasingly attractive in recent years. This is because of the fact that Pion possesses different spin and isotopic spin in comparison to the nucleon. Further the pion upon absorption liberates a good amount of energy, consequently making it sensitive to different aspects of nuclear structure.

In particular, among the pion reactions the (π^+,p) reaction has decided advantages over the rest. In order to effectively use the pion in understanding the nucleus , it is imperative that the reaction studied is not complex enough to complicate the isolation of different effects. In this sense, since the (π^+,p) reaction usually results in a single proton emission in the final state, its kinematical signature is uniquely recognised. Consequently experimental detection and theoretical treatment are straight forward.

Hence, with the advent of meson factories, the reaction has been studied by different authors both experimentally[1-4] and theoretically[5-12]. However there is general disagreement between theory and experiment. This discrepancy can be understood if one considers the absorption by a correlated nucleon. This is because the process in question deals with large momentum transfers (about 400 MeV/c in the forward direction) where the nuclear correlations become important. It is this aspect which motivated us to study this reaction taking into account all the effects such as the initial pion distortion in the presence of nuclear field of the absorbing nucleus prior to its absorption, the correlated wave-functions for the nucleus and the distortion of the emitted proton in the field of the residual nucleus. The study of positive pion absorption by carbon and Lithium are presented in this chapter.

B : THEORY OF PION ABSORPTION

According to the first order time dependent perturbation theory, the differential crosssection for the (π^+,p) process is given by

$$\frac{d\sigma}{d\Omega} = \frac{M}{(2\pi)^2} \frac{k}{q} E_o \sum_f |\langle f|H|i\rangle|^2 \qquad (3.1)$$

where M is the nucleon mass, $\vec{k}$ and $\vec{q}$ are momenta of outgoing proton and incoming pion respectively and E_o is

the total energy of pion. $|i\rangle$ and $|f\rangle$ represent the initial and final states of the system respectively while H is the Galilean-invariant non-relativistic pseudo-scalar-pseudovector interaction (see sec. 20).

$$H = \frac{f}{\mu} \sum_{i=1}^{A} \left[(1-\mu/2M)\, \vec{\sigma} \cdot \overline{\nabla}_{\pi}\, \vec{\tau} \cdot \vec{\phi} - \mu/M\, \vec{\tau} \cdot \vec{\phi}\, \vec{\sigma} \cdot \overline{\nabla}_{N} \right]_i \quad (3.2)$$

Here f is the pion-nucleon coupling constant, $\vec{\phi}$ is the pion field while $\vec{\sigma}$ and $\vec{\tau}$ are the nucleon spin and isospin matrices. $\overline{\nabla}_{\pi}$ acts on the pion field and $\overline{\nabla}_{N}$ acts on the nuclear wavefunction.

The initial state comprises of the positive pion and the absorbing nucleus while the final state is made up of vacuum state of pionic field, the emitted proton and the residual nucleus.

B1. Pion Wavefunction

The incident pion has a kinetic energy of 70 MeV and hence the treatment has to be relativistic. In the absence of any distortion, the pion will be represented by a plane wave. The pion will certainly be distorted due to both the coulomb and the nuclear field of the absorbing nucleus prior to its absorption. Hence the appropriate Klein-Gordon equation has been solved to generate the pion-waves.

The Klein-Gordon equation for stationary eigenstates is obtained from the relativistic energy relation

$$E_o^2 = p^2 + \mu^2 \qquad (3.3)$$

by the prescription $\vec{p} \rightarrow -i\vec{\nabla}$ for the relativistic 3-momentum. Since $\vec{p}$ and E transform as the space and time components of a 4-vector, one includes[13] the electromagnetic scalar potential ϕ and the vector potential $\vec{A}(\vec{r})$ with E and $\vec{p}$ respectively. In this treatment the electromagnetic interaction between π^+ and the nucleus is purely electrostatic and is represented by ϕ with, $\vec{A}(\vec{r})$ being zero.

Then Eq.(3.3) becomes

$$(E_o - V_c)^2 = p^2 + \mu^2 \qquad (3.4)$$

where $V_c = e\phi$. It is now obvious that one cannot add a potential energy term arbitrarily. The Lorentz transformation properties of such terms should be studied first. However since the pion-nucleus optical potential accounting for the strong interaction between them is not completely understood, it has been normally assumed to be a scalar[14] and is included with the energy term E in (3.4).

Consequently $$E \rightarrow E - V_c - V_N \qquad (3.5)$$

Then $$E^2 \rightarrow (E - V_c)^2 - 2EV_N \qquad (3.6)$$

The additional terms $2V_cV_N$ and V_N^2 are arbitrarily dropped from the expression for E^2.

The Klein-Gordon Equation now reads

$$(-\bar{\nabla}^2+\mu^2)\psi = (E_o^2-2V_cE_o+V_c^2 - 2E_oV_N)\psi \qquad (3.7)$$

Expanding ψ in partial waves as

$$\psi = \sum_\ell \frac{u_\ell(r)}{r} i^\ell P_\ell (\cos\theta) \qquad (3.8)$$

and substituting in (3.7) yields the following equation for each partial wave

$$\left[-\frac{1}{r^2}\frac{\partial}{\partial r}\left(r^2\frac{\partial}{\partial r}\right) + \frac{\ell(\ell+1)}{r^2}\right] \frac{u_\ell}{r} P_\ell(\cos\theta)$$

$$= \left[q^2+V_c^2 - 2E_o(V_c+V_N)\right] \frac{u_\ell}{r} P_\ell(\cos\theta) \qquad (3.9)$$

As for the choice of suitable pion-nucleus optical potential, several forms have been proposed in the literature. They include the Standard Kisslinger form[15], the Modified Kisslinger form[16-18] and the Local Laplacian form[19-22]. (Refer sec. 2B for details). They are explicitly given by

Standard Kisslinger Potential :

$$V_N(r) = -Aq^2b_o\rho(r) + Ab_1\,\bar{\nabla}.\rho(r)\,\bar{\nabla} \qquad (3.10)$$

Modified Kisslinger Potential :

$$V_N(r) = -Aq^2b_o\rho(r) + Ab_1\bar{\nabla}.\rho(r)\,\bar{\nabla} - \frac{A}{2}\frac{(T_\pi+\mu)}{M} b_1\bar{\nabla}^2\rho(r) \qquad (3.11)$$

Local Laplacian Potential :

$$V_N(r) = -Aq^2(b_o+b_1)\rho(r) - \frac{A}{2} b_1\,\bar{\nabla}^2\rho(r) \qquad (3.12)$$

where A is the nuclear mass in a.m.u, ρ is the nuclear matter density which is assumed to be spherically symmetric, i.e. $\rho = \rho(r)$. b_o and b_1 are potential parameters which can be related to the pion-nucleon phaseshifts (see sec. 2B).

All these three potentials can be generated with proper choice of constants from the general form

$$2E_o V_N \psi = \left[A_1 \rho + A_2 \, \bar{\nabla}.\rho \, \bar{\nabla} + A_3 \, \bar{\nabla}^2 \rho \right] \psi \qquad (3.13)$$

With this substitution, eqn. (3.9) reduces to the following radial equation for each partial wave

$$(A_2\rho - 1)u_\ell'' + A_2\rho' u_\ell' = \{ \frac{A_2\rho'}{r} + q^2 - 2V_c E_o + V_c^2 - A_3(\rho'' + \frac{2\rho'}{r}) - A_1\rho + \frac{\ell(\ell+1)}{r^2}(A_2\rho - 1) \} u_\ell \qquad (3.14)$$

where the primes denote derivatives w.r.t. r.

This is of the type

$$u_\ell'' + f(r)\, u_\ell' + \left[g(r) - \frac{\ell(\ell+1)}{r^2} \right] u_\ell = 0 \qquad (3.15)$$

with

$$f(r) = \frac{A_2\rho'}{A_2\rho - 1} \qquad (3.16)$$

and

$$g(r) = (1 - A_2\rho)^{-1} \{ \frac{A_2\rho'}{r} + q^2 - 2V_c E_o + V_c^2 - A_3(\rho'' + \frac{2\rho'}{r}) - A_1\rho \} \qquad (3.17)$$

where $f(r)$ and $g(r)$ are complex functions independent of ℓ. This equation (3.15) has been solved to generate the pion

partial waves employing, in turn, the three potentials listed in 3.10-3.12 .

B2. The Nuclear Wavefunction :

It has already been noted that pion upon absorption liberates a great deal of energy with a corresponding high momentum transfer. Hence it is essential that one has a right choice of Nuclear wavefunction which takes into account the short range correlations. We have employed the wavefunction generated by a Hartree-Fock like variational calculation which takes into account central correlations. This is described in section 2D. The wavefunctions in this scheme is given by

$$|\text{Nucleus}\rangle = \sum_m \langle jm\ j\text{-}m|00\rangle\ \psi^{HF}_{\text{neutron}}(jm)\ \psi^{HF}_{c}(j\text{-}m) \qquad (3.18)$$

$$= \sum_m \frac{(-1)^{j-m}}{\sqrt{2j+1}} \sum_n c^{\ell}_{\bar{n}n} |n\ell jm\rangle_{HO}\ \psi^{HF}_{c}(j\text{-}m) \qquad (3.19)$$

$$= \sum_m \frac{(-1)^{j-m}}{\sqrt{2j+1}} \sum_{n\lambda} c^{\ell}_{\bar{n}n} \langle \ell\lambda \tfrac{1}{2}\Lambda | jm\rangle\ |n\ell\lambda\rangle\ \chi_{\frac{1}{2}\Lambda}\ \psi^{HF}_{c}(j\text{-}m) \qquad (3.20)$$

where for spherical HF the summation is restricted only over radial quantum number n and $c^{\ell}_{\bar{n}n}$ are the mixing coefficients. $\langle a\alpha\ b\beta|c\gamma\rangle$ are the Clebsch-Gordan coefficients. ψ^{HF}_{c} represents the nucleus exclusive of π^+ absorbing neutron and χ's are the spin wavefunctions.

B3. The Outgoing Proton Wavefunction :

The emitted proton will be a planewave in the absence of interaction with the residual nucleus. In that case its wavefunction would be

$$\psi_P = e^{i\vec{k}.\vec{r}} \chi_{\frac{1}{2}\Lambda'} \tag{3.21}$$

In actual reality the proton gets distorted due to its interaction with the residual nucleus. The interaction potential between the proton and the residual nucleus is represented by a square well optical potential of radius R_o and strength

$$V = -(U_o + iW_o) \tag{3.22}$$

Since the proton energy is high its distortion is treated in the high energy Glauber approximation[23-25]. Accordingly the proton wavefunction can be written as

$$\psi_P = e^{i\vec{k}.\vec{r}} \exp\left[-\frac{i}{v}\int_o^\infty V(\vec{r} + b\hat{k})\, db\right] \tag{3.23}$$

where v is the proton velocity and $\hat{k}$ is a unit vector in the direction of $\vec{k}$. It has been shown[26] that in effect this modifies the momentum of proton as

$$\vec{k} \rightarrow \vec{k}' = \vec{k}\left(1 + \frac{U_o M}{k^2} - i\frac{W_o M}{k^2}\right) \tag{3.24}$$

and reduces the crosssection by a factor of exp $(-2W_o\bar{R}/k)$

where $\bar{R} = \langle (R_o^2 - r^2\sin^2\theta)^{\frac{1}{2}} \rangle = \frac{3R_o}{4}$, $\theta = (\hat{k},\hat{r})$

Consequently the final state will be represented by

$$|f\rangle = e^{i\vec{k}'.\vec{r}}\ \chi_{\frac{1}{2}\Lambda'}\ D\ \psi_c(j-m') \qquad (3.25)$$

where D is the damping factor given by exp $(-W_o\bar{R}/k)$.

B4. MATRIX ELEMENT

The matrix element is given by

$$\langle f|H|i\rangle = \sum_{n\lambda\Lambda} f/\mu\ \frac{(-1)^{j-m'}}{\sqrt{2j+1}}\ c^{\ell}_{nn}\ \langle \ell\lambda\ \tfrac{1}{2}\ \Lambda|jm'\rangle DF \qquad (3.26)$$

$$F = \langle e^{i\vec{k}'.\vec{r}}\ \chi_{\frac{1}{2}\Lambda'}\ 0|\beta\vec{\sigma}.\vec{\nabla}_\pi\ \vec{\tau}.\vec{\phi}\ -\mu/M\ \vec{\tau}.\vec{\phi}\ \vec{\sigma}.\ \vec{\nabla}_N|$$

free proton

$n\ell\lambda.\ \chi_{\frac{1}{2}\Lambda'}, +\vec{q}\rangle$ distorted pion

bound pion

where $|+\vec{q}\rangle$ denotes a positive pion of momentum $\vec{q}$ while $\langle 0|$ denotes the vacuum state of pion.

The part of the matrix element involving pionic field can be shown to be[27]

$$\langle 0|\vec{\tau}.\vec{\phi}|+\vec{q}\rangle = -\frac{1}{\sqrt{2E_o}}\ \phi(\vec{q},\vec{r})\ \tau_+ \qquad (3.27)$$

where $\tau_+|\text{neutron}\rangle = |\text{proton}\rangle$

and $\phi(\vec{q},\vec{r})$ is given by eq. (3.8).

Then (3.26) becomes

$$\langle f|H|i\rangle = - \sum_{\substack{n\lambda \\ \Lambda L}} \frac{1}{\sqrt{2E_o}} \frac{f}{\mu} \frac{(-1)^{j-m'}}{\sqrt{2j+1}} c^{\ell}_{\overline{nn}} \langle \ell\lambda \tfrac{1}{2}\Lambda | jm' \rangle \; i^{L} DF' \qquad (3.28)$$

$$F' = \langle e^{i\vec{k}'\cdot\vec{r}} \; \chi_{\frac{1}{2}\Lambda'} | \beta \; \vec{\sigma}.\vec{\nabla}_{\pi} \phi - \mu/M \phi \; \vec{\sigma}.\vec{\nabla}_{N} | n\ell\lambda \; \chi_{\frac{1}{2}\Lambda} \rangle$$

Remembering that for any vector $\vec{a}$ [28]

$$\vec{\sigma}.\vec{a} = \Sigma (-1)^{\mu} \sigma_{\mu} a_{-\mu} \qquad (3.29)$$

and

$$\langle \chi_{\frac{1}{2}\Lambda'} | \sigma_{\mu} | \chi_{\frac{1}{2}\Lambda} \rangle = \sqrt{3} \langle \tfrac{1}{2} \Lambda \; 1\mu | \tfrac{1}{2}\Lambda' \rangle \qquad (3.30)$$

with the help of Wigner-Eckart Theorem[29]

and $\vec{a} = \vec{\nabla} \phi$.

With all these substitutions in the matrix element and further evaluation it reduces to

$$\langle f|H|i\rangle = \sum_{\substack{n\lambda\Lambda \\ LL'n'}} 8\pi^2 i^{3L'+L} \left[\frac{3}{2E_o}\right]^{\frac{1}{2}} [f/\mu] \frac{(-1)^{j-m'}}{\sqrt{2j+1}} c^{\ell}_{\overline{nn}}$$

$$\langle \ell\lambda \tfrac{1}{2}\Lambda | jm' \rangle \; A_{\ell\lambda} \; A_{L'n'}{}^{D} \; Y_{L'n'}(\Omega_k)$$

$$[\beta I1 - \mu/M \; I2] \qquad (3.31)$$

where $L'n'$ come from the expansion of proton wavefunctions in partial waves and I1 and I2 are complicated series of terms involving radial and angular integrals. They are too complex to be reproduced here.

$I1 \rightarrow \vec{\nabla}_{\pi}$ acting on the distorted pion wf.

$I2 \rightarrow \vec{\nabla}$ acting on the nuclear wf.

C. CALCULATIONS :

The calculations have been done for the incident pion energy of 70 Mev. This energy was so chosen that it is well below the (3,3) resonance region around 200 Mev so that resonance complexities do not play a role. Further the energy should not be very small that our application of Glauber approximation may cause difficulty. Finally, the experimental results are available which would directly test the theory.

As stated earlier, the pion wavefunctions were generated by solving the Klein-Gordon equation. Since exact analytical solution is not possible, the equation was solved using the fourth-order Runge-Kutta[30] method.

Eq. (3.15) reads

$$u_\ell'' = -f(r)\, u_\ell' + \left[\frac{\ell(\ell+1)}{r^2} - g(r)\right] u_\ell$$

substituting

$$u_\ell' = V_\ell \tag{3.32}$$

this becomes

$$V_\ell' = -f(r)\, V_\ell + \left[\frac{\ell(\ell+1)}{r^2} - g(r)\right] u_\ell \tag{3.33}$$

This is a set of first order coupled equations. Since f and g are complex quantities, in all there are four simultaneous equations. The choice of Runge-Kutta method is because it

provides both the wavefunction and its first derivative at each meshpoint. For solving the Klein-Gordon equation the PIRK[31] code has been employed. As for the potential, three potentials the standard Kisslinger form, the Modified Kisslinger form and the Local Laplacian form have been used. The potential parameters used are the theoretical parameters obtained from pion-nucleon phaseshifts and the best fit parameters obtained by Auerbach[32] (listed in Table 1) to compare the results. The general analysis has been done using the theoretical parameter values. As for the density, the density function generated from the HF type wavefunctions (eq. 3.20) has been used (Appendix B). The coulomb potential has been calculated assuming the nucleus to be spherically symmetric uniform charge distribution. Its form is given by

$$V_c(r) = \frac{Ze^2}{2R_c}\left[3 - (r/R_c)^2\right] \qquad r \leq R_c$$
$$= \frac{Ze^2}{r} \qquad r \geq R_c \qquad (3.34)$$

where Z is the nuclear charge and R_c is the charge radius of the nucleus. The values of R_c for both the nuclei are as got from the electron scattering data.

The oscillator well parameter α $\left(= \sqrt{\frac{M\omega}{\hbar}} \right)$ is taken to be 125 Mev, a value obtained from electron scattering[33,34] experiments and proton scattering experiments[35]. The coefficients c^{ℓ}_{nn} used in the nuclear wavefunction are listed

in Table 2. The proton optical well parameters are taken from a compilation by Peray et al.[36,37]. However there are uncertainties in the values of these parameters and hence we have varied the parameters within allowed range to study the differential crosssection. The justification for using the square well has been discussed in the next section.

D RESULTS AND DISCUSSION :

The positive pion absorption by carbon-12 and Lithium-6 systems have been studied. The crosssections have been calculated separately for pion absorption by $0s_{\frac{1}{2}}$ neutron and $0p_{\frac{3}{2}}$ neutron. The investigative analysis include the relative importance of pion distortion, nuclear correlations and proton distortion, the sensitivity of the crossection with respect to certain parameters like the oscillator well parameter α, the proton potential parameters U_o, W_o etc, ambiguity in the interaction vertex, the qualitative and quantitative differences in the crosssection when the three kinds of pion distortion are employed and the relative importance of the pion-nucleus optical potential from the point of view of pion absorption. The results have been separately analysed for the two nuclei.

D1. CARBON-12

The initial crosssection for this reaction which employed plane waves for both the pion and the proton with neutron represented by the Harmonic oscillator wavefunction were an order of magnitude less than the experimental value. However they exhibited a high degree of sensitivity with variation in α, the oscillator well parameter. Within allowable range the crosssection was uncertain by a factor varying from eight to almost three orders of magnitude depending upon the proton emission angle. Such fluctuations result if α is varied between the minimum value of 120 Mev obtained from electron scattering data[34] to 135 Mev, a value obtained from proton scattering experiments.[35] By employing the correlated wavefunction for the nucleus and taking into account the pion and proton distortion, we find that the crosssection is very much stabilised with a variation of just 15 per cent.

The differential crosssection has been calculated using both the theoretical values for the potential parameters b_o, b_1 obtained from pion-nucleon phaseshifts and the best fit parameters obtained by Auerbach et al.[32]. These are compared in Fig. 1. It is seen that while this change does not produce any noticeable difference in the behaviour with angle, it does indeed reduce the crosssection by about

FIG 1 : Angular distribution of the crosssection for the reaction $^{12}C(\pi^+,p)^{11}C$ using Standard Kisslinger Potential: Comparison between theoretical (TH) and the best fit (FT) parameter values for b_o and b_1 (Table 1 for values).

FIG 2 : Comparison of angular distribution of crosssection for absorption by $Op_{3/2}$ and $Os_{1/2}$ neutron. Pion waves distorted by the Standard Kisslinger Potential.

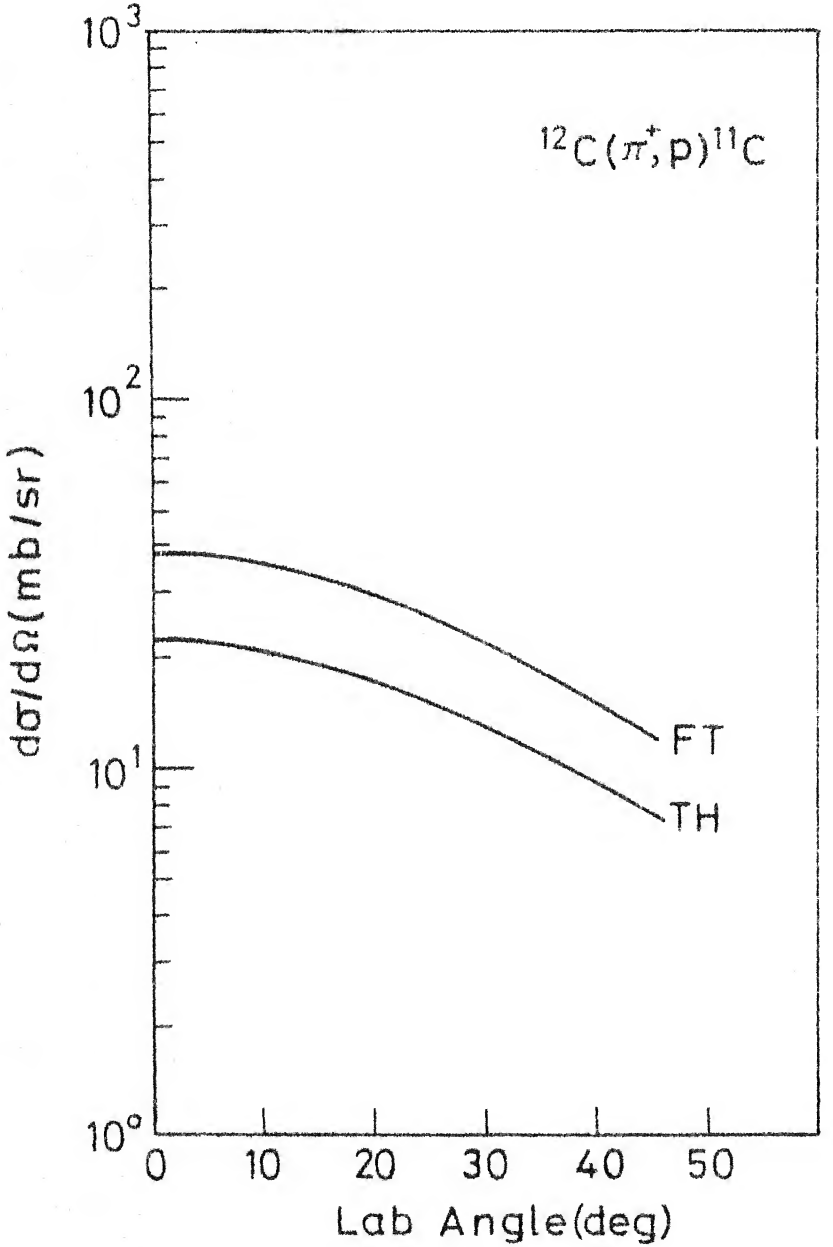
10^3
10^2
10^1
10^0
$^{12}C(\pi^+,p)^{11}C$
FT
TH
$d\sigma/d\Omega$(mb/sr)
0
10
20
30
40
50
Lab Angle(deg)

FIG.1

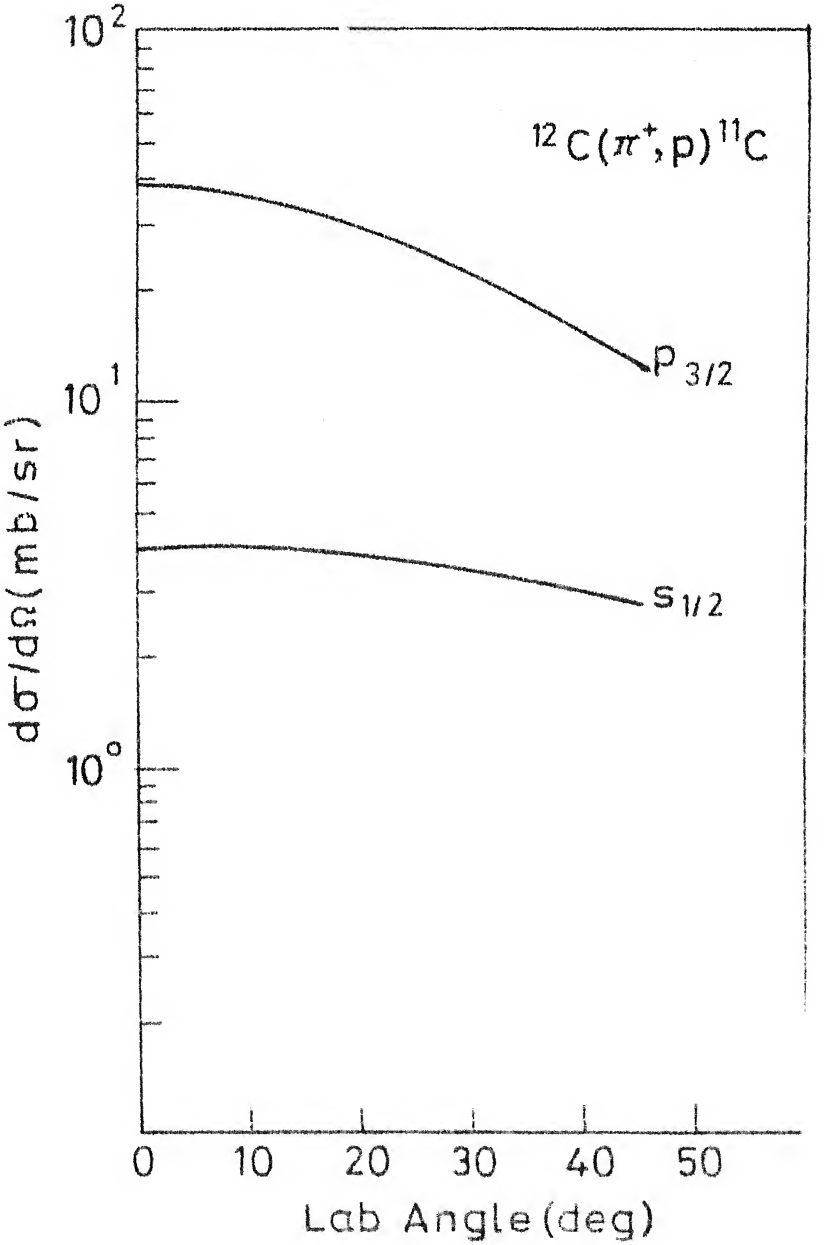
10^2
10^1
10^0
$^{12}C(\pi^+,p)^{11}C$
$P_{3/2}$
$S_{1/2}$
$d\sigma/d\Omega$(mb/sr)
0
10
20
30
40
50
Lab Angle(deg)

FIG. 2

50 per cent. This implies that it is very essential to employ the right set of parameters. Incidentally this difference is comparable to the maximum difference occuring between the theory and fit values in the π - ^{12}C elastic scattering at 69.5 Mev[32].

In Figs. 2-4 the differential crosssection for absorption by $Op_{\frac{3}{2}}$ neutron is compared with that of absorption by $Os_{\frac{1}{2}}$ neutron. The $Os_{\frac{1}{2}}$ crosssection is found to be lower than the $Op_{\frac{3}{2}}$ case by a factor ranging from 6 to 9 depending upon the type of potential used to generate the pion distorted waves.

As already been pointed out, the final state interaction has been tackled assuming a complex square well (eq. 3.22). Since the value for ^{11}C at the concerned energy is not available, the values of ^{12}C has been employed for the proton optical parameters U_o and W_o. Even for ^{12}C there are sizable uncertainities in the values and hence the variation of the crosssection with U_o, W_o, the square well parameters has been studied. They are exhibited in Fig. 5. It is found that the crosssections are practically insensitive to the variations in U_o and W_o within allowed range.

The differential crosssection obtained from the three kinds of distorted pion waves are compared in Fig. 6. It is seen that while modified Kisslinger results are of the same

FIG 3 : Comparison of angular distribution of crosssection for absorption by $op_{3/2}$ and $os_{1/2}$ neutron. Pion waves distorted by the Modified Kisslinger Potential.

FIG 4 : Comparison of angular distribution of crosssection for absorption by $op_{3/2}$ and $os_{1/2}$ neutron. Pion waves distorted by the Local Laplacian Potential.

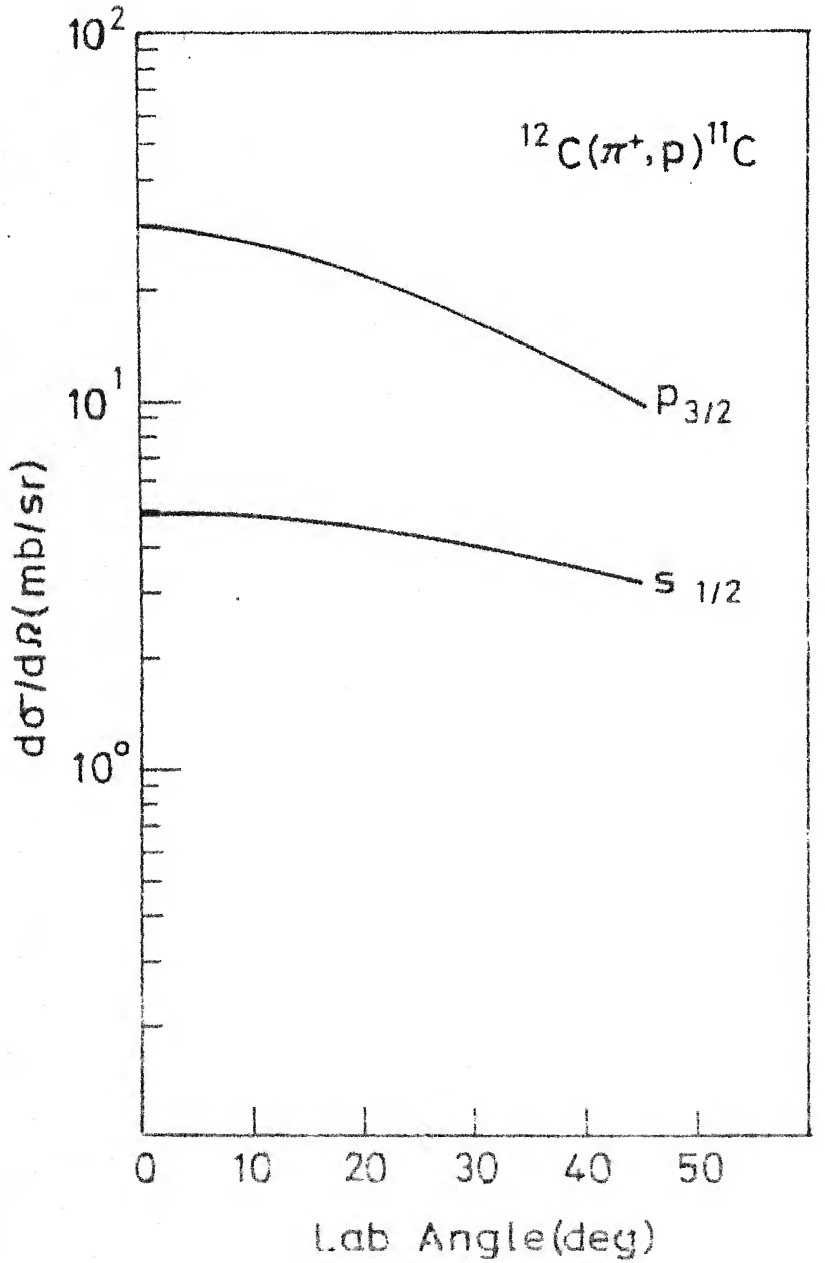
10^2
10^1
10^0
$^{12}C(\pi^+,p)^{11}C$
$P_{3/2}$
$S_{1/2}$
$d\sigma/d\Omega$(mb/sr)
0
10
20
30
40
50
Lab Angle(deg)

FIG. 3

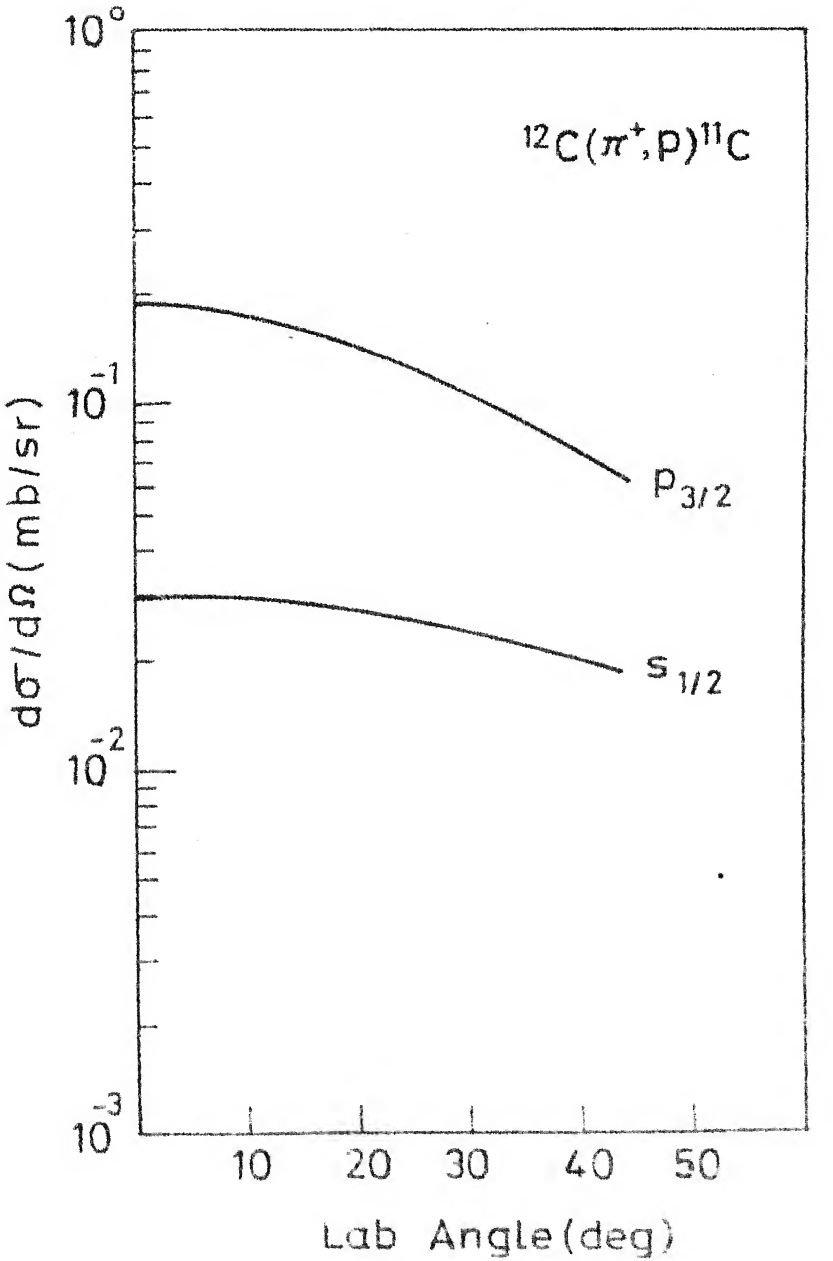
10^0
10^{-1}
10^{-2}
10^{-3}
$^{12}C(\pi^+,p)^{11}C$
$P_{3/2}$
$S_{1/2}$
$d\sigma/d\Omega$(mb/sr)
10
20
30
40
50
Lab Angle(deg)

FIG. 4

FIG 5 : Study of the variation of differential crosssection for the reaction $^{12}C(\pi^{+},p)^{11}C$ with proton optical well parameters. Pion waves distorted by the Standard Kisslinger form. Proton optical well parameters in units of Mev:

Curve A : $U_o = 9$ $W_o = 15$

Curve B : $U_o = 10$ $W_o = 20$

Curve C : $U_o = 12$ $W_o = 25$

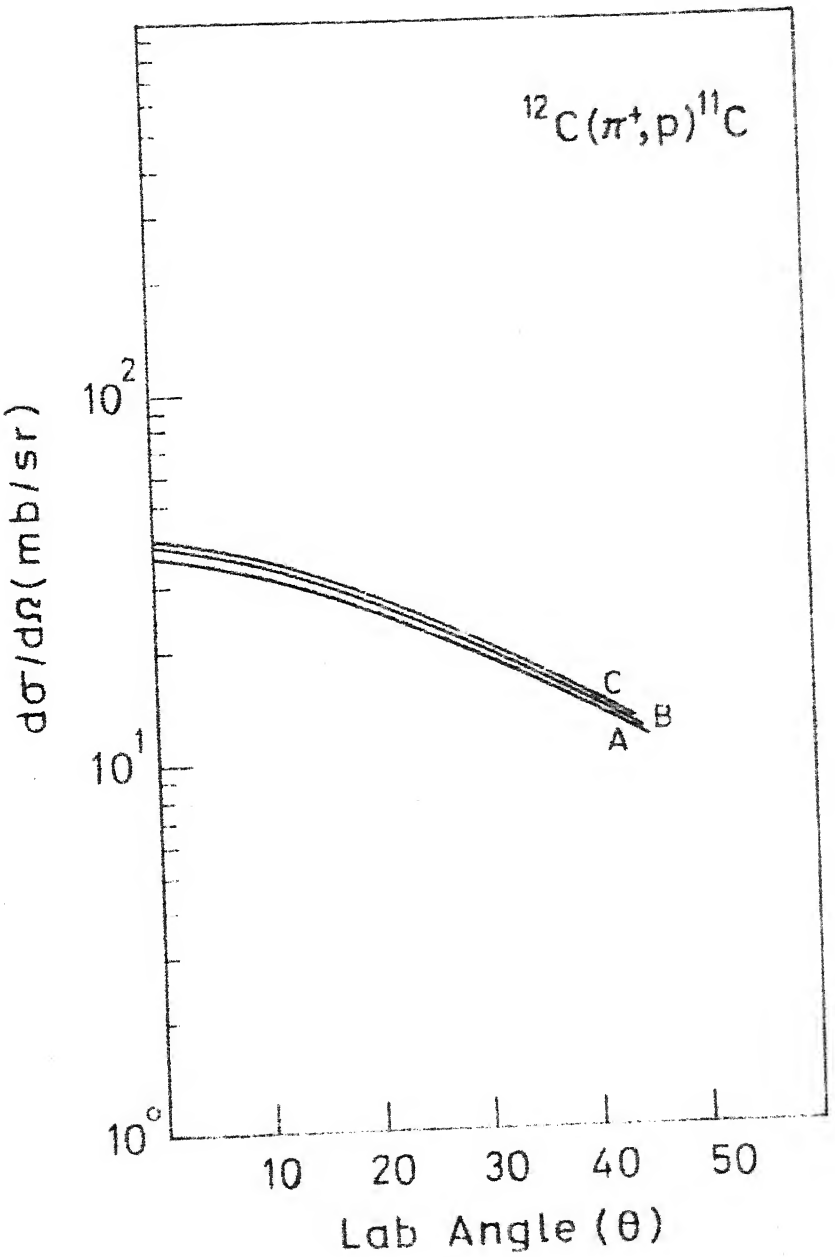
$^{12}C(\pi^+,p)^{11}C$
$d\sigma/d\Omega$ (mb/sr)
10^2
10^1
10^0
C
B
A
10
20
30
40
50
Lab Angle (θ)

FIG. 5

FIG 6 : Comparison of the differential crosssection for the reaction $^{12}C(\pi^{+},p)^{11}C$ with the three kinds of pion distortion.

SK : Standard Kisslinger potential.

MK : Modified Kisslinger potential.

LL : Local Laplacian potential.

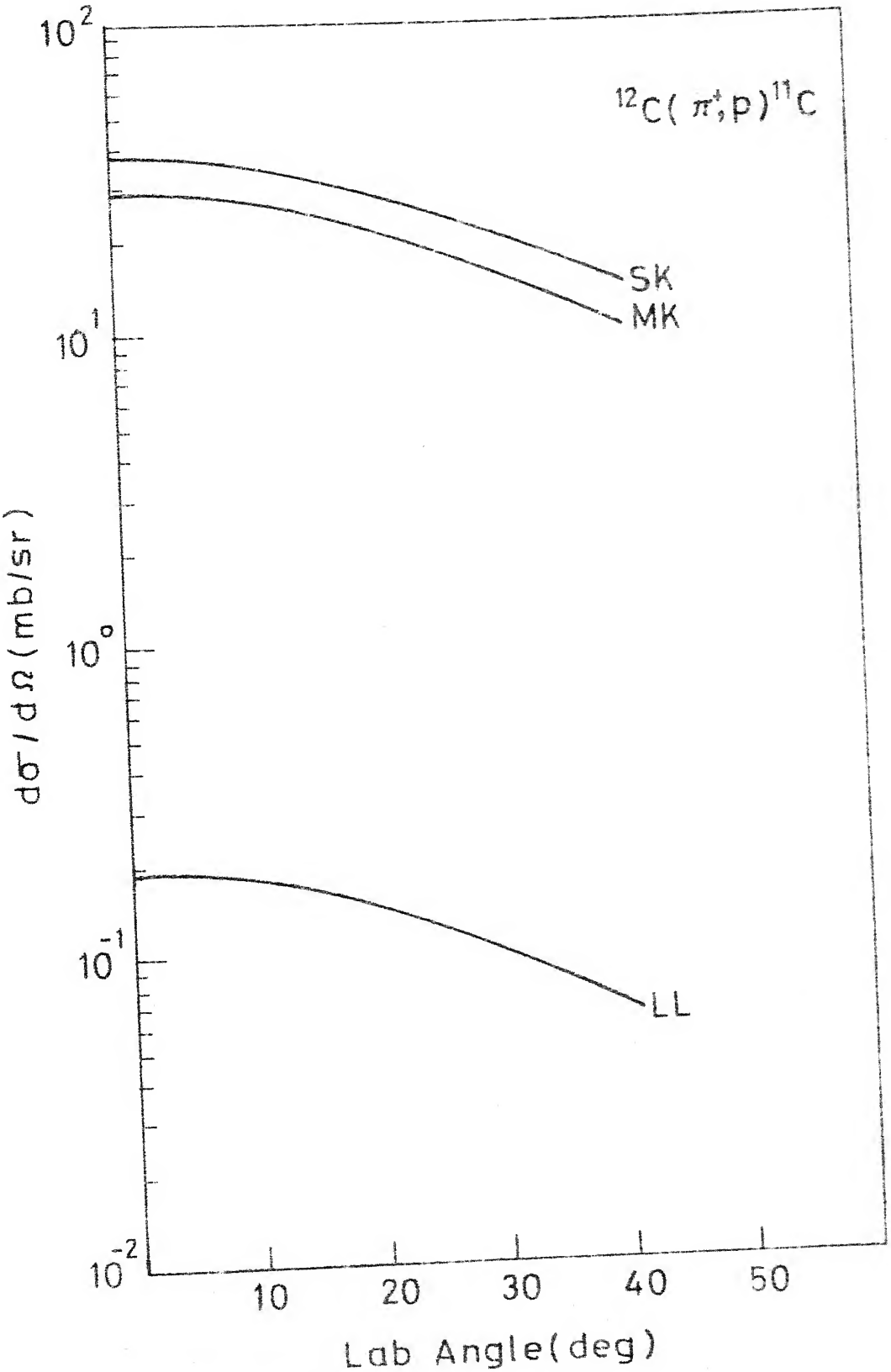
10^2
$^{12}C(\pi^+,p)^{11}C$
SK
MK
10^1
10^0
10^{-1}
LL
10^{-2}
$d\sigma/d\Omega$ (mb/sr)
10
20
30
40
50
Lab Angle(deg)

FIG. 6

order as that of standard Kisslinger model, magnitude wise it is slightly lower. On the other hand, employing the pion distortion by the Local potential lowers the crosssection by two orders in comparison with Standard Kisslinger results. However the behaviour with the angle is almost same. A detailed discussion about the likely cause of this is provided at the end of Lithium-6 analysis.

Finally the calculated crosssection is compared with the experimental results[3] in Fig. 7. The differential cross-section corresponding to Standard Kisslinger potential and Modified Kisslinger potential are higher than the experimental results by two orders of magnitude, nearly. But the cross-sections employing the pion waves generated by the Local Laplacian potential reproduce the correct order of magnitude. However while it matches with the experimental values for $\theta \geq 20^{\circ}$ it is lower than the measured values for $\theta = 0^{\circ}$ and $\theta = 11^{\circ}$. Incidentally it should be noted that the measurements for $\theta = 0^{\circ}$ and 11° are done by different experimental groups. (Ref 1-3).

D2. LITHIUM-6 :

The crosssection for this reaction was calculated because experimental data is available, making possible comparison with the theory. In fact Amato et al.[3] have measured $^{6}Li(\pi^{+},p)^{5}Li$ differential crosssection at 68 Mev systematically for a number

FIG 7 : Comparison of the differential cross-section for the reaction $^{12}C(\pi^+,p)^{11}C$ with experimental data.

Curve A : Standard Kisslinger results.

Curve B : Modified Kisslinger results.

Curve C : Local Laplacian results.

JE[7] : Calculations by Jones and Eisenberg.

WK[10] : Calculations by Wienke.

EL[5] : Calculations by Leutournex and Eisenberg.

RK[9] : Calculations by Rost and Kunz.

MP[11] : Calculations by Miller and Phatak

Curves JE and RK have a normalisation factor 10 and 80-160 respectively.

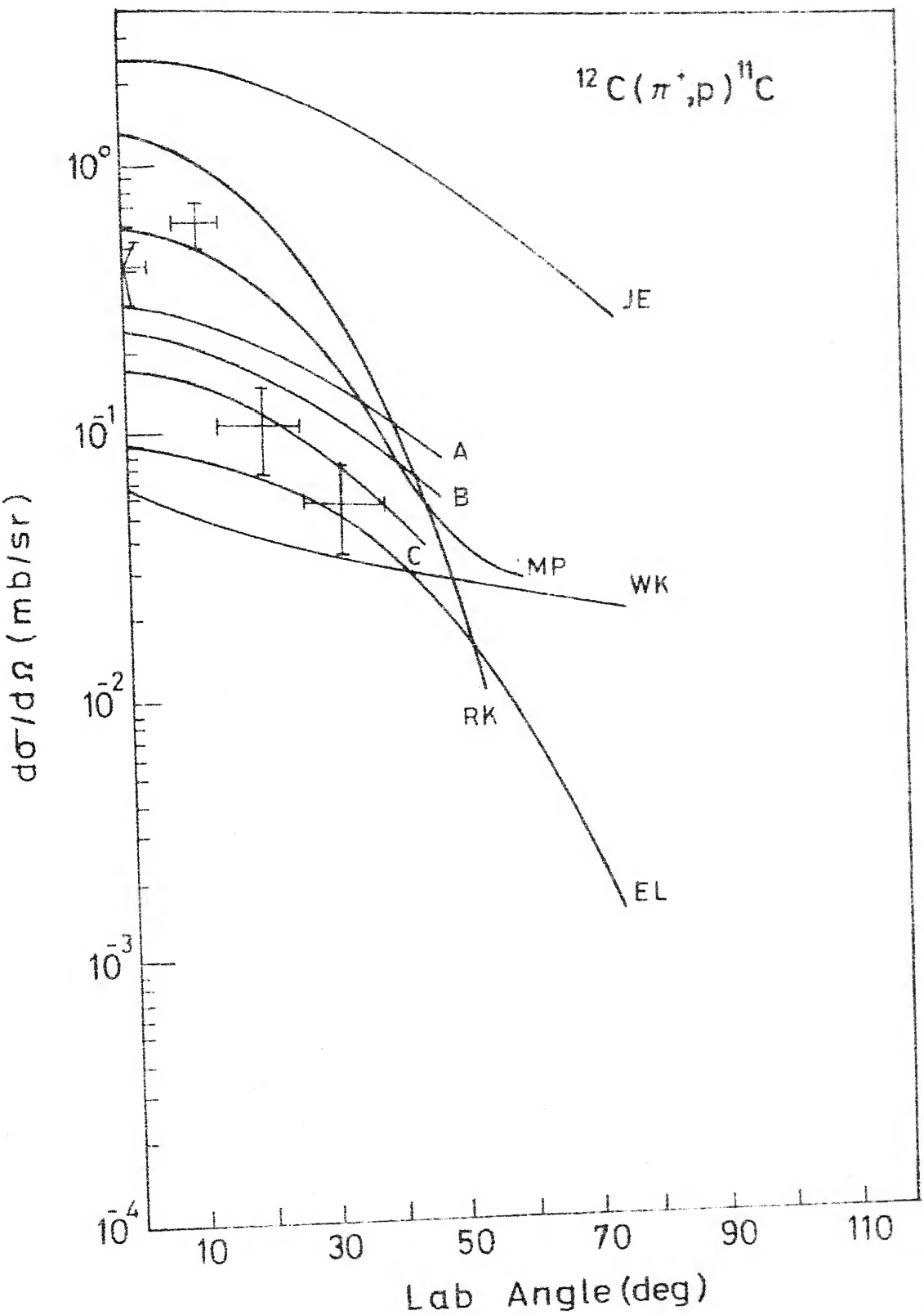
$^{12}C(\pi^+,p)^{11}C$
10^0
10^{-1}
10^{-2}
10^{-3}
10^{-4}
$d\sigma/d\Omega$ (mb/sr)
JE
A
B
C
MP
WK
RK
EL
10
30
50
70
90
110
Lab Angle (deg)

FIG. 7

of angles between 30° and 90°. Further, so far only one theoretical calculation has been done on ^{6}Li. This calculation by Wienke[38] employes a field theoretic method with pion and proton represented by plane waves while the neutron is represented by Harmonic oscillator with exponential tails. The pion rescattering has also been taken into account which prevents the crosssection from falling with angle rapidly.

The availability of experimental result over a wide range of angle in comparison with ^{12}C has motivated us to do a systematic analysis of various effects on ^{6}Li. The calculations in the case of Lithium have been done using theoretical values for the π-potential parameters b_0 and b_1. Attempts to produce best fit parameters failed[32].

There has been certain ambiguity[19,39] about the interaction vertex particularly over the inclusion of the term $-\mu/2M$ in the coefficient of $\bar{\nabla}_{\pi}$ (eq. 3.2). It has been found by our calculation that the difference between the two cases produce only a change of about 16 per cent in the calculated crosssection both at 0° and at 90°. This is in contrast with the results which dont take into account pion distortion and nuclear correlations producing 35 per cent change.

The variation of the crosssection with α, the oscillator well depth parameter comes out to be about 25 per cent a figure higher than the carbon results, but considerably lower than the earlier results. The likely cause is discussed at the end.

Figs. 8-10 exhibit the variation of differential crosssection with U_o, W_o the proton optical well parameters. This variation is very small. Similar to the case of carbon, the variation is negligible.

The differential crosssection has been calculated using in turn pion waves generated from the three potentials. The results are presented below separately.

1. Standard Kisslinger Form

Fig. 11 exhibit the crosssection for pion absorption by Lithium when the standard Kisslinger potential (eq. 3.10) is employed. The calculation includes pion and proton distortion together with nuclear correlations (curve A) It is actually two orders of magnitude higher than the experimental value. In the same figure the relative importance of pion distortion, nuclear correlations and the proton distortion are studied. Curve B is obtained by switching off the pion distortion due to the strongfield of the absorbing nucleus. However this takes into account the coulomb distortion and the finite size of the nucleus. This lowers

FIG 8 : Study of the variation of differential crosssection for the reaction $^{6}Li(\pi^{+},p)^{5}Li$ with proton optical well parameters. Pion distorted by the Std. Kisslinger Form. In units of Mev,

Curve A $U_o = 9$, $W_o = 15$

Curve B $U_o = 10$, $W_o = 20$

Curve C $U_o = 12$, $W_o = 25$.

FIG 9 : Study of the variation of differential crosssection for the reaction $^{6}Li(\pi^{+},p)^{5}Li$ with proton optical well parameters. Pion distorted by the Modified Kisslinger form.

In units of Mev,

Curve A $U_o = 9$, $W_o = 15$

Curve B $U_o = 10$, $W_o = 20$

Curve C $U_o = 12$, $W_o = 25$.

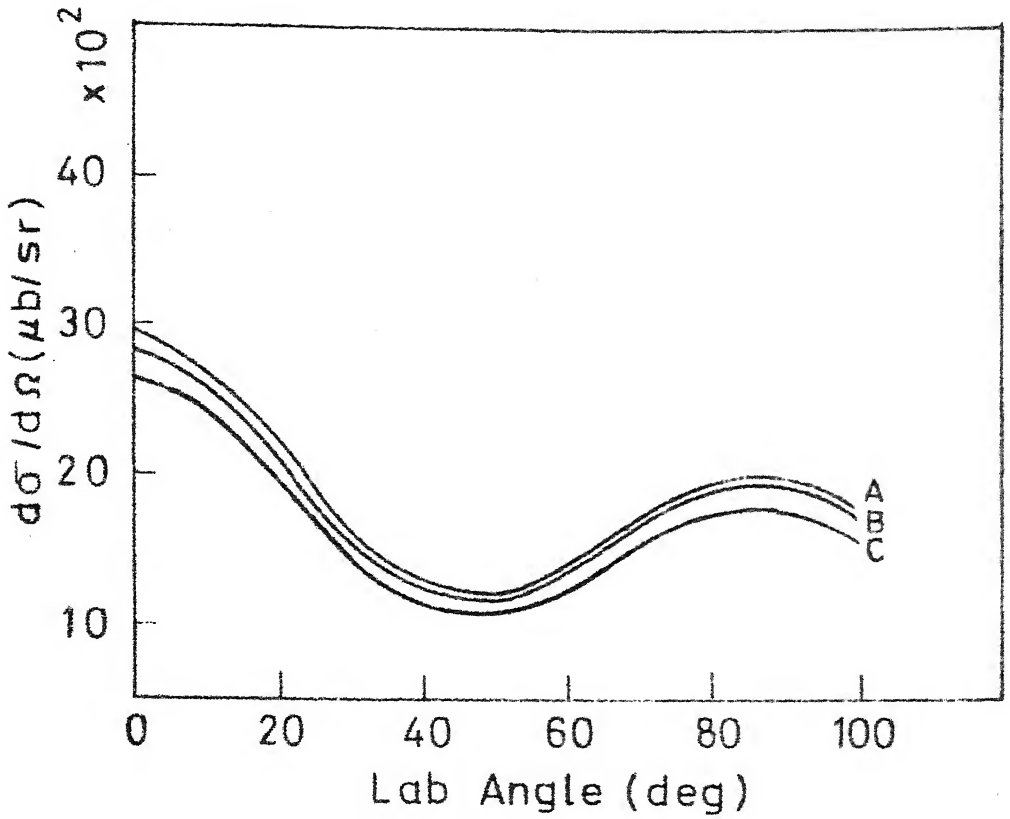
dσ/dΩ(μb/sr) x10²
40
30
20
10
0
20
40
60
80
100
Lab Angle (deg)
A
B
C

FIG. 8

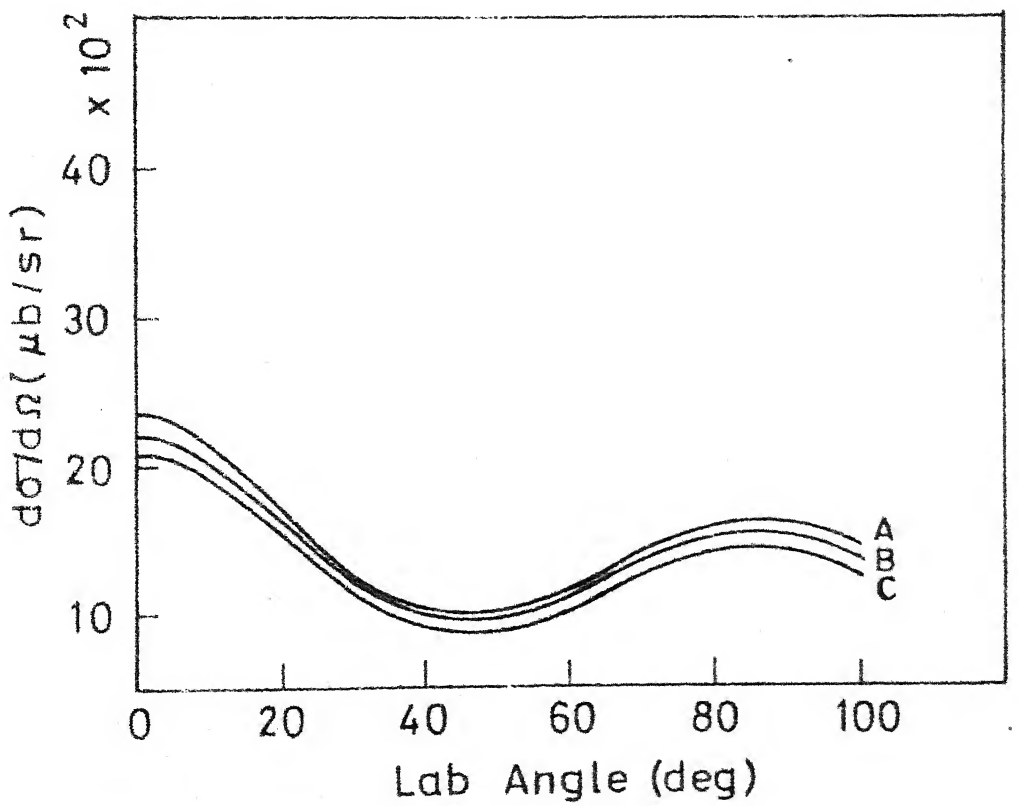
dσ/dΩ(μb/sr) x10²
40
30
20
10
0
20
40
60
80
100
Lab Angle (deg)
A
B
C

FIG.9

FIG 10 : Study of the variation of differential crosssection for the reaction $^{6}Li(\pi^{+},p)^{5}Li$ with proton optical well parameters.
Pion distorted by the Local Laplacian form.
In unit of Mev,

Curve A : $U_o = 9$, $W_o = 15$

Curve B : $U_o = 10$, $W_o = 20$

Curve C : $U_o = 12$, $W_o = 25$.

FIG 11 : Angular distribution for the reaction $^{6}Li(\pi^{+},p)\ ^{5}Li$. Study of relative importance of pion distortion, Nuclear correlations and proton distortion.
Pion distorted by the Standard Kisslinger Potential.

Curve A : All effects included.

Curve B : Pion distortion by strong field excluded (scaled)

Curve C : Nuclear correlations excluded. [Right a
Scal

Curve D : Proton distortion excluded.

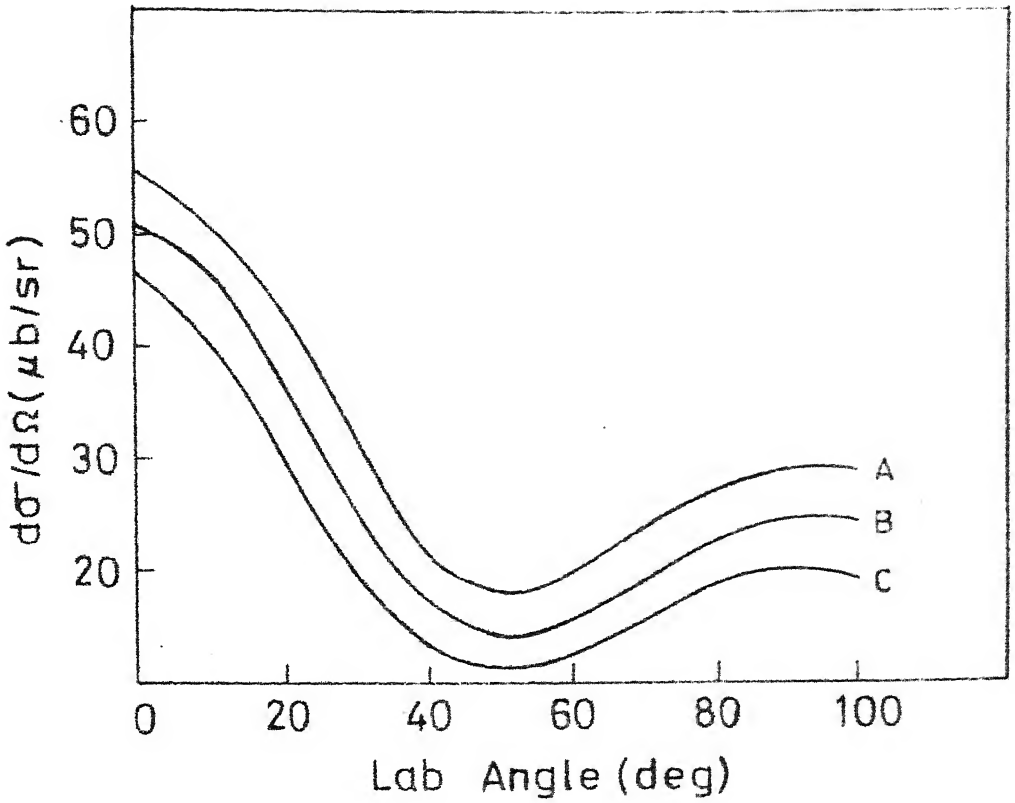
60
50
40
30
20
dσ/dΩ(μb/sr)
A
B
C
0
20
40
60
80
100
Lab Angle (deg)

FIG.10

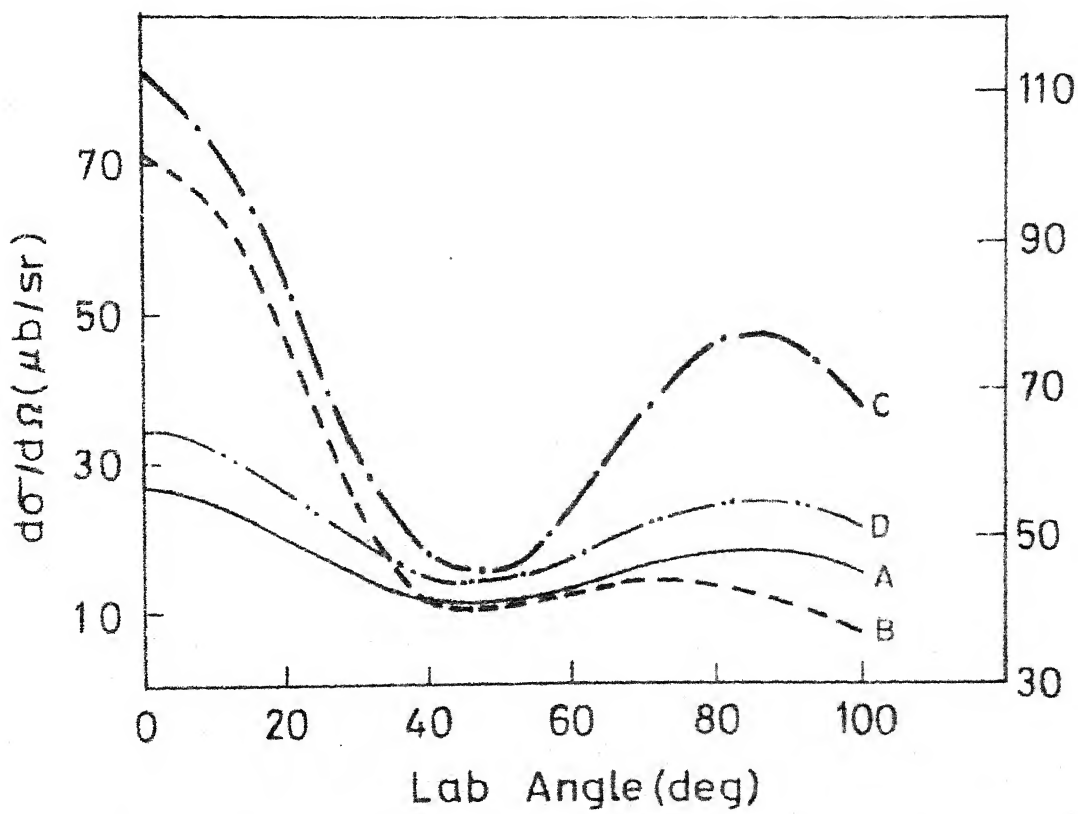
70
50
30
10
dσ/dΩ(μb/sr)
110
90
70
50
30
C
D
A
B
0
20
40
60
80
100
Lab Angle (deg)

the crosssection by a factor of 500 (curve B scaled in the graph). Secondly the effect of peaking in the forward direction is enhanced. Curve C results when only the nuclear correlations are neglected. This reduces the cross-section (in comparison with curve A). Further this enhances the forward peaking but equally causes an increase for $\theta > 60^{\circ}$. Curve D represents the cross-section when one ignores the outgoing proton distortion. Here again the crosssection shows an increase in magnitude. These curves indicate that pion distortion is very important. Further for the correct behaviour the correlations are equally important. For, the experimental results indicate that the crosssections vary slowly with angle for $\theta \geq 60$. This effect is given by including the Hartree-Fock wavefunctions. In this context it is well to remember that the correlated wavefunctions enter into the formalism explicitly through nuclear wave-functions and as a density function in the pion-nucleus optical potential. Inclusion of the correlations stabilises the behaviour for $\theta > 60^{\circ}$.

The interaction vertex between the pion and the nucleon (Eq. 3.2) comprises of two terms, one dependent upon the gradient of pionic field and the other dependent upon the pionic field. Barnhill[39] has pointed out that there is ambiguity regarding the coefficient of the second term i.e. $\bar{\nabla}_N$ term. In Fig. 12 the effect of these two terms are

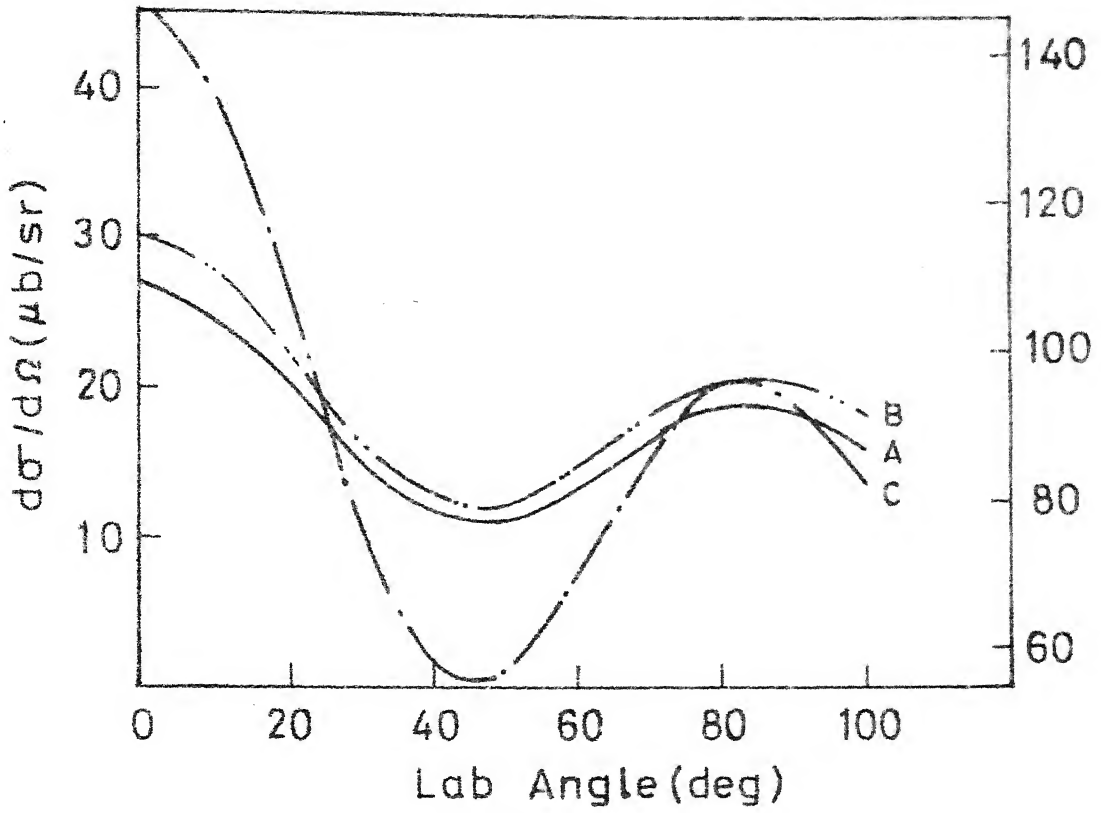
dσ/dΩ (μb/sr)
40
30
20
10
140
120
100
80
60
B
A
C
0
20
40
60
80
100
Lab Angle (deg)

FIG. 12

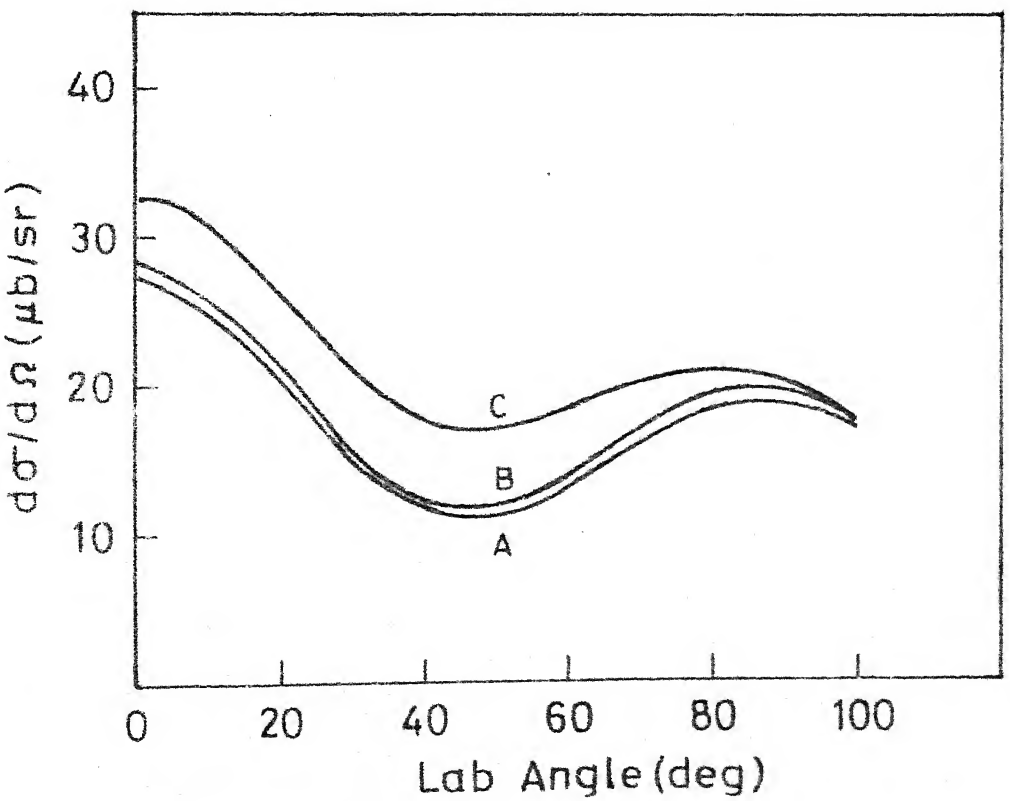
dσ/dΩ (μb/sr)
40
30
20
10
C
B
A
0
20
40
60
80
100
Lab Angle (deg)

FIG. 13

investigated. Curve A is the actual crosssection plotted for reference. Curve B represents the crosssection with $\bar{\nabla}_N$ term neglected. This therefore includes only $\bar{\nabla}_\pi$ term. It is seen that the crosssection registers a slight increase while orderwise it is the same as curve A. On the other hand if one includes only the $\bar{\nabla}_N$ term the crosssection decreases by two orders of magnitude (curve C - scaled in the fig.) emphasising the dominance of $\bar{\nabla}_\pi$ term over the $\bar{\nabla}_N$ term.

The pion nucleus optical potential used to generate the pion waves consists of two terms: the s-wave term and the p-wave term. The relative importance of these two terms from the point of view of (π^+,p) differential reaction is studied in Fig. 13. Curve A represents the actual cross-section. Curve B is the result of switching off the s-wave term. Therefore it includes only the p-wave term. The effect is a slight increase in the magnitude. On the other hand if the p-wave term is suppressed the crosssection falls down by two orders of magnitude (curve C scaled in the figure). This very clearly emphasises the dominance of the p-wave term over the s-wave term.

2. MODIFIED KISSLINGER FORM

When one employs the modified Kisslinger potential (eq. 3.11) to generate the pion-waves, the behaviour of (π^+,p) crosssection is very similar to that obtained from

FIG 14 : Angular distribution for the reaction $^{6}Li\ (\pi^{+},p)^{5}Li$ using Modified Kisslinger Potential. Study of relative importance of pion distortion, Nuclear correlations and proton distortion.

Curve A : All effects included.

Curve B : Pion distortion by strong field excluded (curve scaled).

Curve C : Nuclear correlations excluded.

Curve D : Proton distortion excluded.

FIG 15 : Angular distribution for the reaction $^{6}Li\ (\pi^{+},p)^{5}Li$ using Modified Kisslinger potential. Study of the relative importance of the two terms in the pion-nucleon interaction vertex.

Curve A : With both terms present.

Curve B : With only $\bar{\nabla}_{\pi}$ term present.

Curve C : With only $\bar{\nabla}_{N}$ term present. [Right axis scale]

FIG 16 : Angular distribution for the reaction $^{6}Li\ (\pi^{+},p)^{5}Li$ using Modified Kisslinger potential. Study of the relative importance of the s-wave term and the p-wave term in the pion nucleus optical potential.

Curve A : With both terms included.

Curve B : With only p-wave interaction.

Curve C : With only s-wave interaction (scaled).

FIG. 17 Angular distribution of the crosssection for the reaction $^{6}Li(\pi^{+},p)^{5}Li$ using Local Laplacian potential. Study of relative importance of pion distortion, Nuclear correlations and proton distortion.

Curve A : All effects included.

Curve B : Pion distortion by strongfield excluded (curve scaled).

Curve C : Nuclear correlations excluded.

Curve D : Proton distortion excluded.

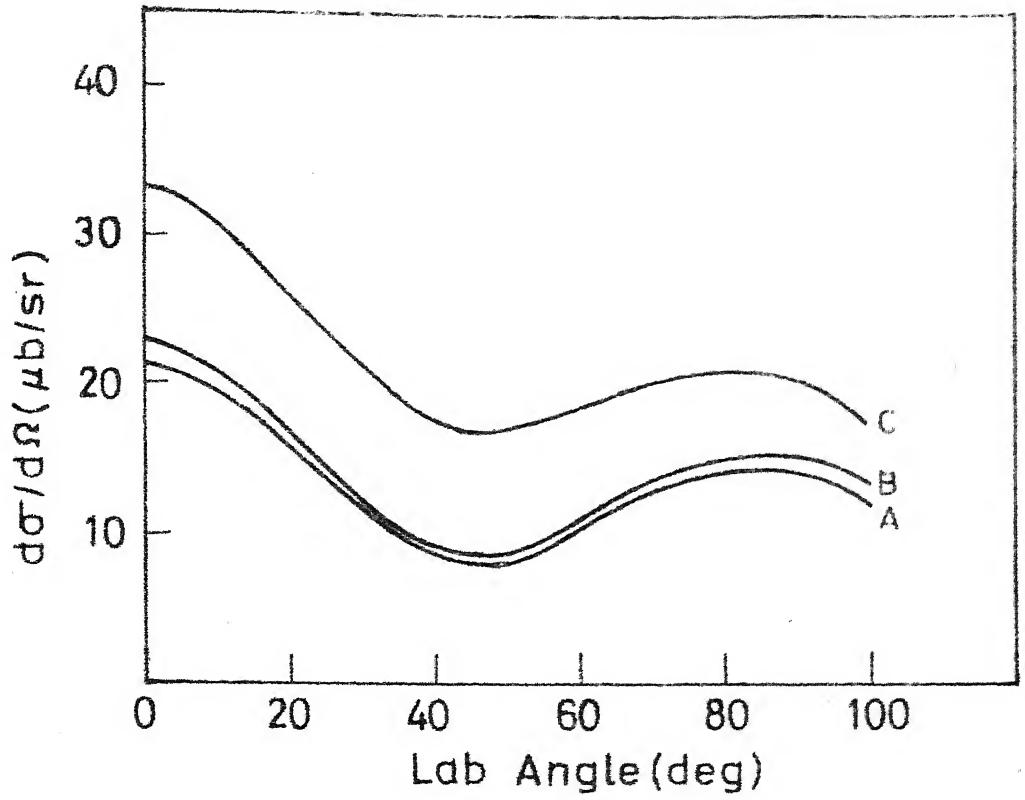
40
30
20
10
dσ/dΩ(μb/sr)
C
B
A
0
20
40
60
80
100
Lab Angle(deg)

FIG.16

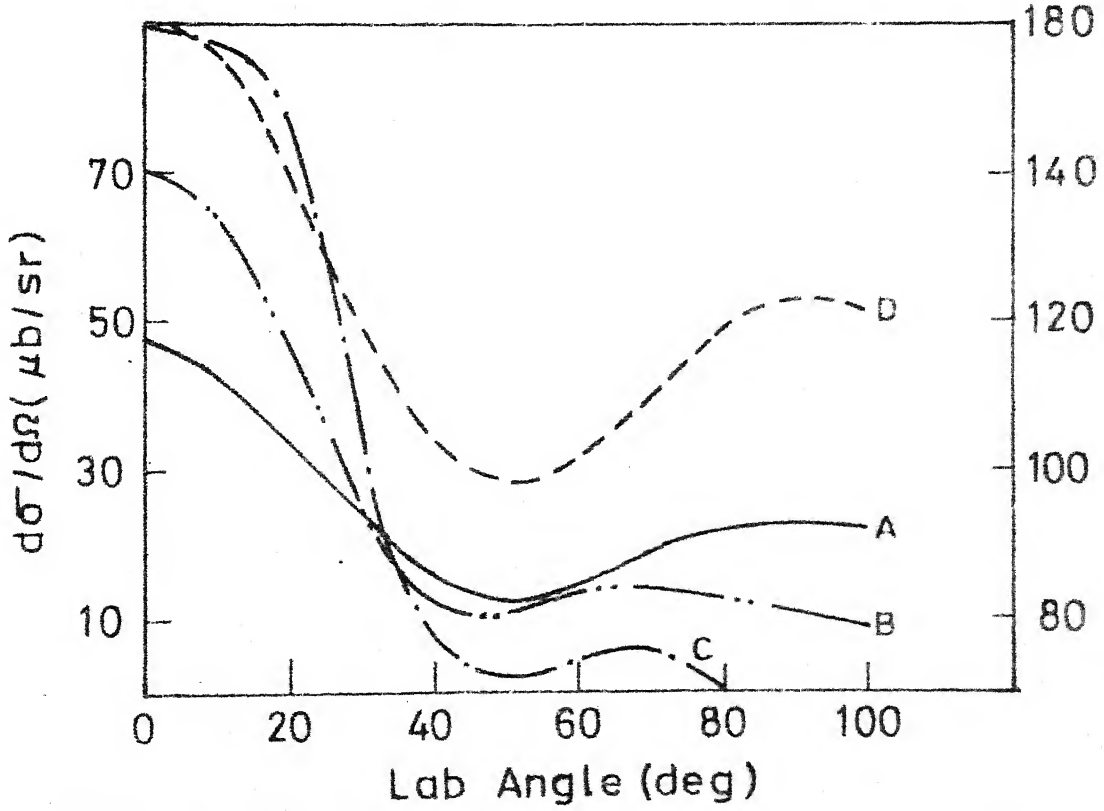
180
140
120
100
80
70
50
30
10
dσ/dΩ(μb/sr)
D
A
B
C
0
20
40
60
80
100
Lab Angle (deg)

FIG.17

crosssection got from other potentials, the relative difference between curve B and curve C is not as prominent as the other two cases (Figs. 12 and 15). The crosssection with only $\overline{\nabla}_N$ term included is small compared to the actual crosssection by a factor of 4 only.

Fig. 19 studies the relative importance of the two terms in the Local Laplacian form. If the s-wave term is neglected then the crosssection (curve B) is increased and equally the peaking in the forward direction is enhanced. This is in contrast to the curves obtained in the other two cases (compare figs. 12 and 15). In fact this feature of the Local Laplacian form gets reflected in the actual cross-section (curve A). On the other hand, when only the s-wave term is included there is a reduction in the crosssection together with the suppression of peaking effect in the forward direction.

Thus the analysis with different potentials imply that the p-wave part is the more dominant of the two terms. Further it also establishes the importance of pion distortion and nuclear correlations.

Finally the calculated crosssections are compared with the experimental data in Fig. 21. The crosssections are two orders of magnitude higher than the experimental value when one employs either Standard Kisslinger potential or Modified

FIG 18 : Angular distribution for the reaction $^{6}Li(\pi^{+},p)^{5}Li$ using Local Laplacian Potential. Study of the relative importance of the two terms in the pion-nucleon interaction vertex.

Curve A : With both terms present.

Curve B : With only $\bar{v}_{\pi}$ term present.

Curve C : With only $\bar{v}_{N}$ term present (scaled).

FIG 19 : Angular distribution for the reaction $^{6}Li\ (\pi^{+},p)^{5}Li$ using Local Laplacian Potential. Study of the relative importance of the s-wave term and the p-wave term in the pion-nucleus optical potential.

Curve A : With both terms present.

Curve B : With only b_{1} term.

Curve C : With only b_{o} term (scaled).

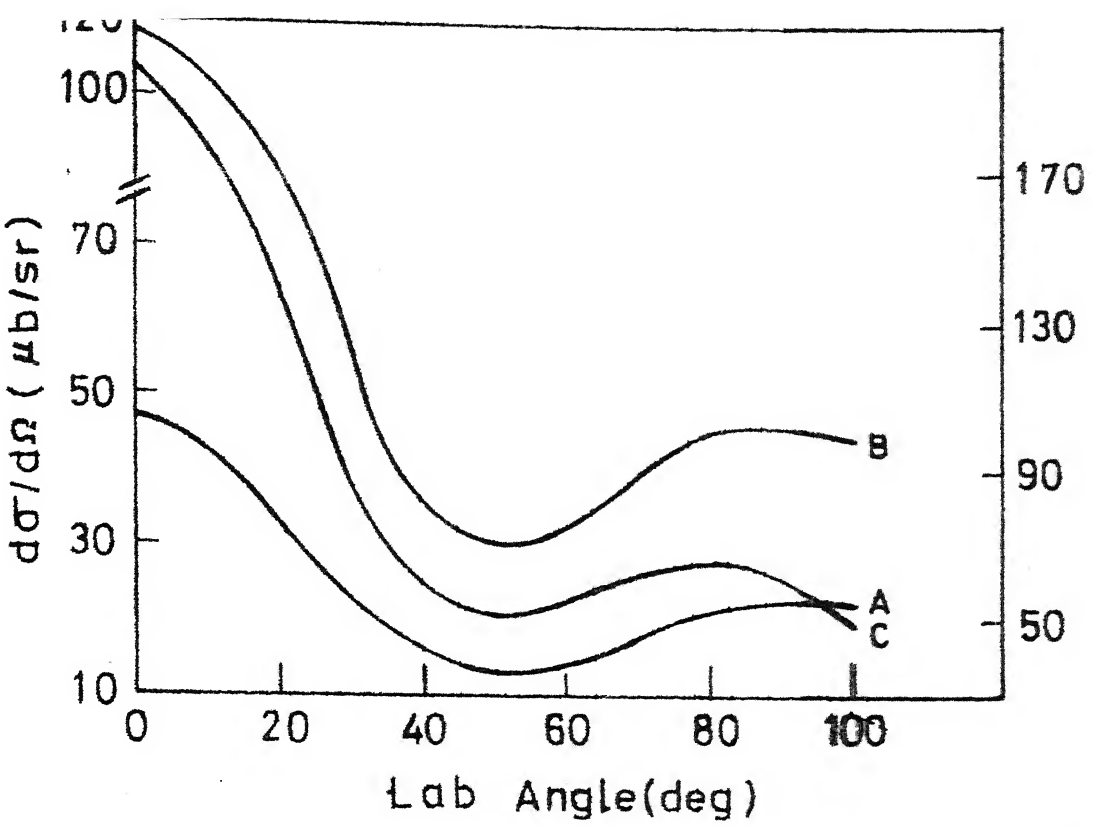
100
70
50
30
10
dσ/dΩ (μb/sr)
170
130
90
50
B
A
C
0
20
40
60
80
100
Lab Angle(deg)

FIG.18

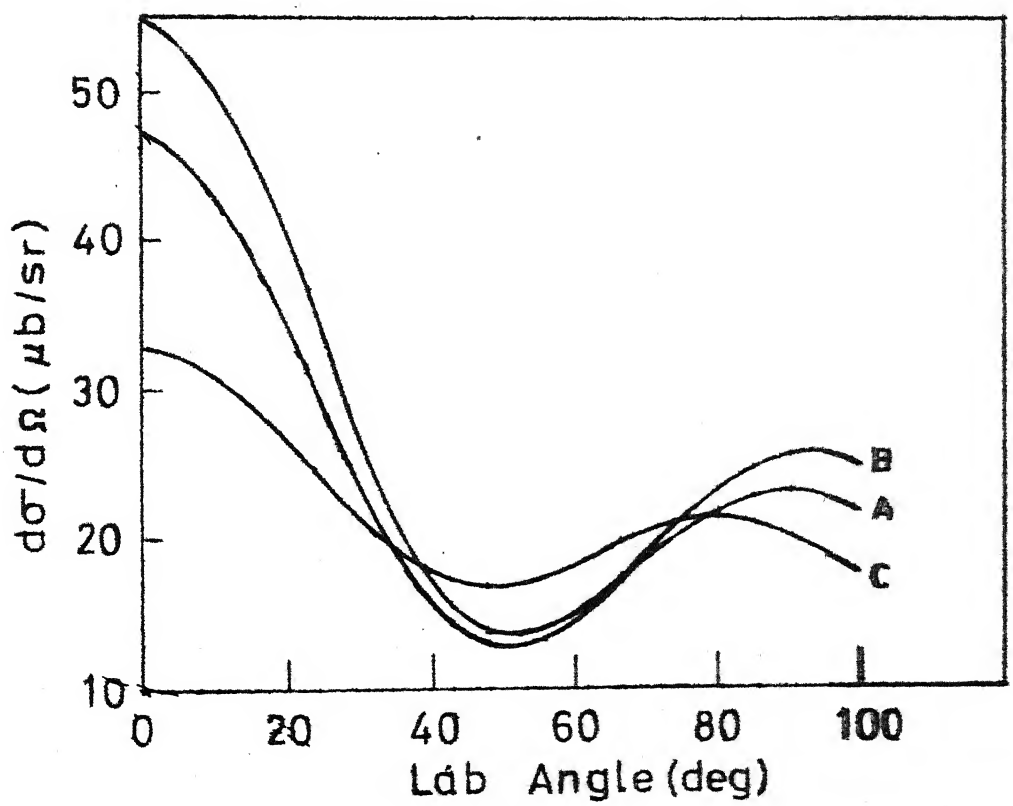
50
40
30
20
10
dσ/dΩ (μb/sr)
B
A
C
0
20
40
60
80
100
Lab Angle (deg)

FIG.19

FIG 20 : Comparison of the differential crosssection for the reaction $^{6}Li\ (\pi^{+},p)^{5}Li$ with the three kinds of pion distortion.

K : Standard Kisslinger potential (scaled)

M : Modified Kisslinger Potential (scaled)

LL : Local Laplacian potential.

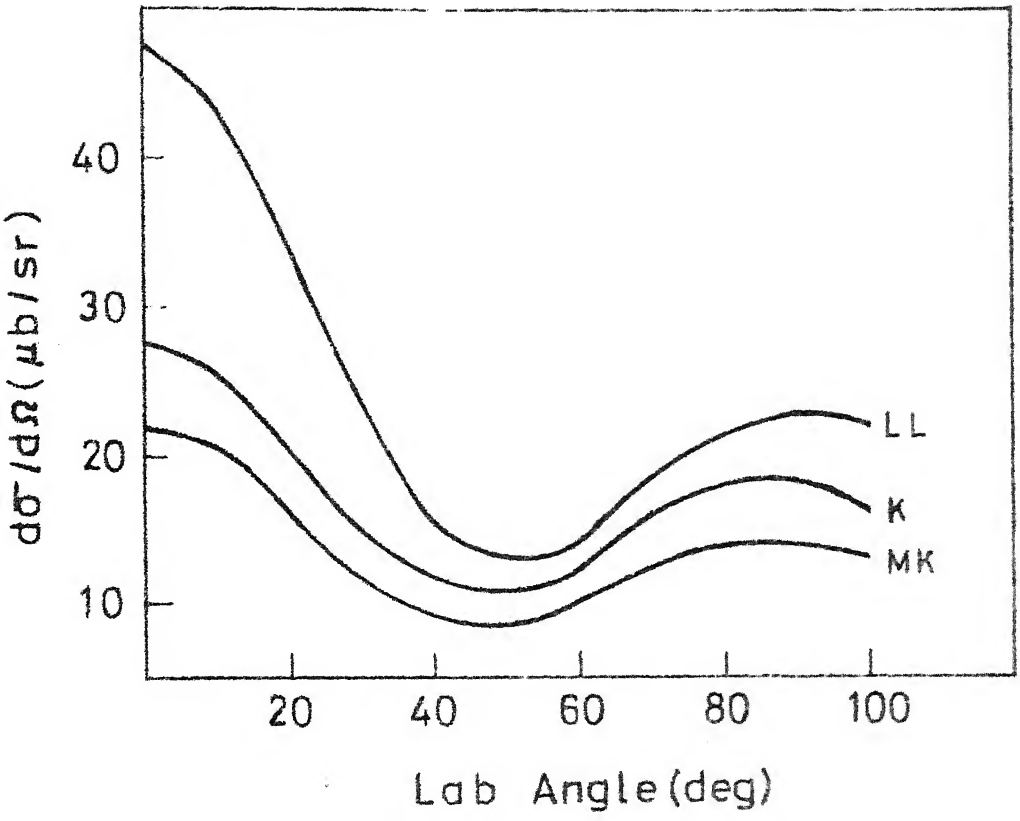

FIG. 20

FIG 21 : Comparison of the differential cross-section for the reaction $^{6}Li(\pi^{+},p)^{5}Li$ with the experimental data.

Curve A : Results with Modified Kisslinger Potential (scaled)

Curve B : Results with Standard Kisslinger Potential (scaled).

FIG 22 : Comparison of the differential crosssection for the reaction $^{6}Li\ (\pi^{+},p)^{5}Li$ with experimental data. Smooth curve (—) is the result obtained by employing Local potential to distort pion waves. Dashed (----) curve is that obtained by Wienke.[38]

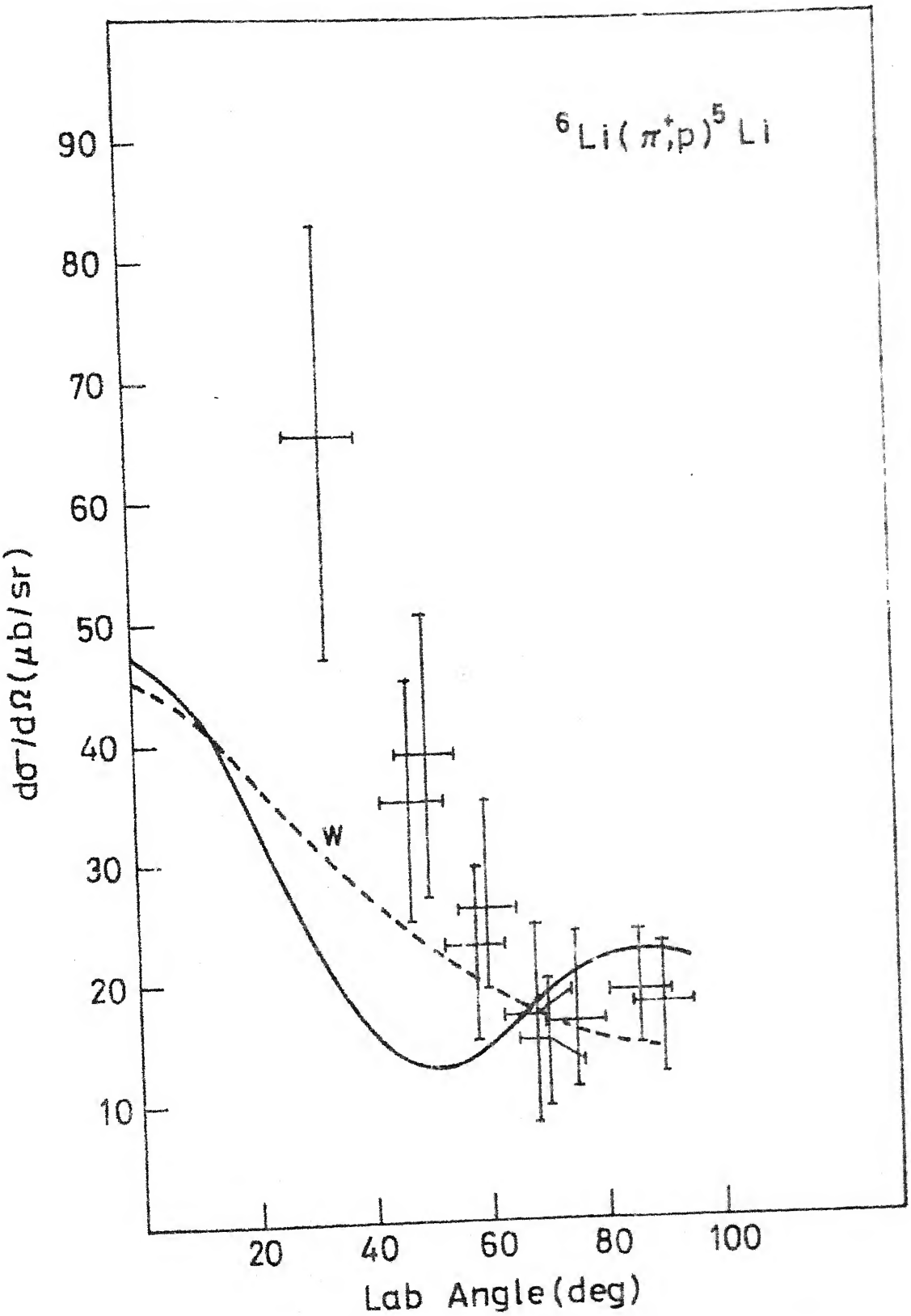
$^6Li(\pi^+,p)^5Li$
90
80
70
60
50
40
30
20
10
dσ/dΩ(μb/sr)
W
20
40
60
80
100
Lab Angle(deg)

dominant in comparison with the s-wave term. Further when one puts off the p-wave term the crosssection falls by two orders of magnitude implying that the p-wave term is over dominant. On the other hand in the case of Local Laplacian case even though it is dominant it is not as dominant. In the interaction term eq. 3.2 the importance of ∇_π term has already been seen. Thus the pion waves generated by the inclusion of non-local term together with $\nabla_\pi \phi$ term in the interaction vertex are responsible for the enhanced cross-section in the case of standard Kisslinger potential and Modified Kisslinger Potential. In fact with these two potentials the pion distortion gets over emphasised.

The shifting of minima in the case of Lithium and other possible discrepancies like, a slightly higher variation in the crosssection with α, in comparison with the carbon-results are possibly due to the nuclear wave function which is employed for Lithium-6. Strictly speaking the formalism from which these nuclear wavefunctionsare generated (sec 2D) are applicable only to closed shell or closed sub-shell nuclei. But Li^6 belongs to neither category. The $C^{\ell}_{\bar{n}n}$'s for Lithium were generated by assuming a spherically symmetric HF field. These calculations are similar to that of ^{6}He which has $0s_{\frac{1}{2}}$ level completely filled and $0p_{\frac{3}{2}}$ exactly half filled.

This is confirmed by the preliminary results from the calculations of $^{16}O(\pi^+,p)^{15}O$ reaction using this Hartree-Fock formalism which is presently being carried out[40]. In this spherical nuclear case, the calculations yield a minima around 80^o consistent with experimental results. This is further borne out by the fact that in the case of Helium (chapter 4) the employment of this HF formalism yield a minima at 80^o.

A complex square well has been employed to treat the pion-nucleus scattering. Strictly speaking, the potential is not expected to plunge to zero abruptly. But the proton energy being large, the absorption is expected to be more or less uniform throughout the volume. Again the details of the nuclear surface are expected to play an important role only for large Z where coulomb repulsion is more effective. Moreover the spin-orbit term is just about 2-3 MeV at the proton energy considered[7]. Consequently we believe that the error due to square well is small.

E. CONCLUSIONS :

The present analysis of (π^+,p) reaction with carbon and Lithium leads to the following conclusions.

1. All the three effects like pion distortion, nuclear correlations and final state proton distortion are important in general.

2. In the presence of pion distortion and HF wavefunctions for the nucleus, the undesirable sensitivity of the crosssection with parameters like the oscillator well depth parameter α, disappears. Equally, the crosssections are stabilised with respect to the proton optical parameters. The ambiguity over the inclusion of the term $-\mu/2M$ in the interaction vertex does not seem to affect the pion absorption crosssection.

3. The crosssection is sensitive to the kind of pion distortion one employes. The crosssections are nearly two orders of magnitude higher than the experimental values if Standard Kisslinger Potential/Modified Kisslinger potential is employed. With these potentials, the importance of pion distortion seems to be overemphasised. On the other hand employing the Local potential results in a crosssection closest to the experimental value.

Table 1

PION OPTICAL POTENTIAL PARAMETERS(a

Nucleus	Re b_o	Im b_o	Re b_1	Im b_1	Remarks
^{12}C	-0.66	0.41	6.30	1.30	Theoretical Values T_π = 69.5 Mev
^{12}C	-2.30	0.73	6.81	0.93	Best Fit Values Std. Kisslinger Form T_π = 69.5 Mev
^{6}Li	-0.39	0.43	6.22	1.79	Theoretical Values T_π = 78 Mev.

(a Reference : Auerbach et. al.[32]

Table 2

EXPANSION COEFFICIENTS $C^{\ell}_{\bar{n}n}$

Nucleus	$os_{\frac{1}{2}}$ neutron			$op_{\frac{3}{2}}$ neutron		
	n=1	n=2	n=3	n=1	n=2	n=3
^{6}Li	0.9691	-0.1362	0.2059	0.8726	0.4831	0.0724
^{12}C	0.9397	0.3139	0.1359	0.9647	0.2140	0.1532

REFERENCES :

1. T.R. Witten, M. Blecher and K. Gotow, Phys. Rev. 174 (196

2. K. Gotow in High Energy Physics and Nuclear Structure III 1969 ed, S. Devons (Plenum, N.Y, 1970), P. 374.

3. J. Amato, R.L. Burman, R. Macek, J. Oostens, W. Shlaer, E. Arthur, S. Sobottka and W.C. Lam, Phys. Rev. C9 (1974) 501.

4. D. Bachelier, J.L. Boyard, T. Hennino, J.C. Jordain, P. Radvanyi and M. Roy-Stephan, Phys. Rev. C15 (1977) 2139.

5. J. LeTournex and J.M. Eisenberg, Nucl. Phys. 87 (1966) 33

6. R.S. Kaushal and Y.R.Waghmare, Phys. Lett. B31 (1970) 637

7. W.B. Jones and J.M. Eisenberg, Nucl. Phys. A154 (1970) 49

8. R.S. Kaushal, Lett. Nuovo Cim. 1 (1971) 793.

9. E. Rost and P.D. Kunz, Phys. Lett. B43 (1973) 17.

10. B.R. Wienke, Prog. Theo. Phys. 49 (1973) 1220.

11. G.A. Miller and S.C. Pathak, Phys. Lett. B51 (1974) 129.

12. R.S. Bhalerao and Y.R. Waghmare, Pramāna (India) 5 (1975) 154.

13. L.I. Schiff, Quantum Mechanics, 3rd Edition, Mc-Graw Hil N.Y. (1968) ch. 13.

14. W.F. Baker, J. Rainwater and R.E. Williams, Phys. Rev. 11 (1958) 1763.

    W.F. Baker, J. Rainwater and H. Byfield, ibid. 112 (1958) 1773.

15. L.S. Kisslinger, Phys. Rev. 98 (1955) 761.

16. H.K. Lee and H. McManus, Nucl. Phys. A167 257.

17. G. Faldt, Phys. Rev. C5 (1972) 400.

18. J.H. Koch and M. Sternheim, Phys. Rev. C6 (1972) 1118.

CHAPTER 4

POSITIVE PION ABSORPTION BY HELIUM-4

A. INTRODUCTION

B. THEORY OF PROTON DISTORTION

C. THEORY OF PION ABSORPTION

D. CALCULATIONS

E. RESULTS AND DISCUSSION

REFERENCES

CHAPTER 4

POSITIVE PION ABSORPTION BY HELIUM-4

A. INTRODUCTION

The importance of pion distortion and nuclear coorelations in the reaction $^{Z}A(\pi^{+},p)\ ^{Z}A-1$ was already seen in the analysis with Lithium and Carbon nuclei. Further, the inclusion of these effects reproduced the behaviour of angular distribution of the crosssection with reasonable success. In this context, it should be noted that the radial Hartree-Fock formalism[1] which has been employed to take into account correlations should indeed work well with the Helium system. This is because of its being the lightest spherical nucleus. It is these considerations which provided the necessary motivation to study the positive pion absorption by Helium-4 with the emission of a single nucleon. Even though experimental results are not available for this reaction, the results are compared, using the principle of detailed balancing, with the (p,π^{+}) reaction.

This study of $^{4}He(\pi^{+},p)\ ^{3}He$ reaction takes into account the pion distortion, nuclear correlations and the proton distortion. The pion distortion includes both coulombic and nuclear distortion effects. The nuclear wavefunctions

are generated by a radial Hartree-Fock calculation assuming a spherically symmetric HF field for the Helium-nucleus. These are similar to the formalism employed in the previous chapter. In the case of proton distortion two different approaches have been employed. This has been done with a two-fold objective: (i) to study the importance of proton distortion on the crosssection and (ii) to isolate any characteristic features induced by employing the high energy Glauber approximation and a complex square well.

In the first approach, the proton distortion has been included through the high energy approximation employing for the proton-nucleus optical potential, a complex square well. The formalism here is basically the same as that considered in the study of Carbon and Lithium systems. In the second approach, starting from fundamental nucleon-nucleon interaction, a proton-He^3 potential has been constructed through a variational calculation. This is described below.

B THEORY OF PROTON DISTORTION

The manybody Schrodinger equation is given by

$$\{ \Sigma\ T_i + V_{\text{Many body}} \} \psi = E \psi \quad . \qquad (1)$$

Difficulties in solving this equation are two-fold

1. Need to know the correct V.
2. Even if V were known (suppose) then only approximate methods are available to solve this Schrodinger eqn.

As for the first, one normally starts with two-body forces assuming that three and higher body forces are absent. Thus

$$V = \sum_{\substack{i,j \\ i \neq j}} \frac{1}{2} V_{ij} \qquad (2)$$

As for the second, the approximate methods available are few. Out of them methods like Born approximation, Perturbation theory etc. involve the smallness of certain parameters for validity. But the variational method does not involve any such constraint and is hence preferred here.

In this approach, the proton-He^3 system is considered as a two cluster problem. This method is similar to the one-channel approximation in Resonating group method[2] as applied by Tang et. al.[3,4] but with some fundamental assumptions. Firstly it is assumed that the residual Helium-3 system is at rest which is not strictly correct. Secondly the outgoing proton wavefunction is not antisymmetrized with respect to nucleons of He^3. This is justified on the grounds that the outgoing proton has a large energy in comparison with the average energy of nucleons in Helium-3. The basic steps involved are a right choice of trial wavefunction, choice of the interaction Hamiltonian (with a

suitable choice of nucleon-nucleon interaction), application of the variational method, and the solution of the resulting equation for generating the proton wavefunctions.

B1 Wavefunction

The trial wavefunction chosen to represent the nucleons of He^3 is a single gaussian. Thus the wavefunction of the cluster is given by

$$\phi = \exp\{-\frac{1}{2}\bar{\alpha}\sum_{i=1}^{3} r_i^2\} F(\vec{R}) \quad \xi_{s\sigma} \qquad (3)$$

where $F(\vec{R})$ is the outgoing proton wavefunction and $\xi_{s\sigma}$ is the spinpart. The choice of gaussian form is to facilitate the solution of integrals analytically. The value of $\bar{\alpha}$ (bar employed to distinguish it from the oscillator well depth parameter used elsewhere) has been fixed so as to reproduce the correct r.m.s. radius for Helium-3. This yields a value $0.36\ F^{-2}$ for $\bar{\alpha}$.

B2 Interaction Potential

The nucleon-nucleon interaction potential chosen is a pure two-body central potential of gaussian form. However the fact that they differ in the singlet and triplet state is taken into account. This choice of pure central potential is to facilitate computation.

The potential is given by

$$V_{ij} = \left[\frac{1}{2}(1+P^{\sigma}_{ij})\,V_t + \frac{1}{2}(1-P^{\sigma}_{ij})\,V_s\right]\frac{1}{2}(1+P^{r}_{ij}) + \frac{e^2}{4r_{ij}}\{(1+\tau_{iz})(1+\tau_{jz})\} \quad (4)$$

where $V_t = -V_{ot}\exp\left[-\kappa_t r^2\right]$ and $V_s = -V_{os}\exp\left[-\kappa_s r^2\right]$ (5)

P^{σ}_{ij} and P^{r}_{ij} are spin and space exchange operators respectively and τ corresponds to isospin.

B3 The Method

The total Hamiltonian for the system is given by

$$H = \frac{-\hbar^2}{2M}\sum_{i=1}^{4}\nabla_i^2 + \sum_{i>j}^{4} V_{ij} \quad (6)$$

The wavefunctions are determined from the variational equation

$$\langle\delta\phi|\,H-E\,|\phi\rangle = 0 \quad (7)$$

This being the scattering problem, one varies the relative wavefunction of proton $F(\vec{R})$ itself[5]. It should be remembered that variation in $F(\vec{R})$ and $F^*(\vec{R})$ are independent. One then expands the proton wavefunction in partial waves as

$$F(\vec{R}) = \sum_{\ell}\frac{f_\ell(R)}{R}P_\ell(\cos\theta) \quad (8)$$

Upon substituting it in eqn. (7) and solving all the necessary integrals analytically one gets the following differential equation for each partial wave.

$$f_\ell'' + \left[A_t e^{-B_t R^2} + A_s e^{-B_s R^2} - \frac{C}{R} - \frac{D}{R^2} + K^2 \right] f_\ell = 0 \qquad (9)$$

with

$$A_t = -(2M/\hbar^2)\left[V_{ot} \left(\frac{\alpha}{\alpha+\kappa_t}\right)^{3/2} \right] \qquad (10)$$

$$B_t = \kappa_t - \kappa_t^2/(\alpha + \kappa_t)$$

$$A_s = -(4M/\hbar^2)\left[V_{os} \left(\frac{\alpha}{\alpha+\kappa_s}\right)^{3/2} \right] \qquad (11)$$

$$B_s = \kappa_s - \kappa_s^2/(\alpha + \kappa_s)$$

$$C = 4Me^2/\hbar^2$$

$$D = \ell(\ell+1) \qquad (12)$$

substituting $n_\ell = f_\ell'$ (13)

eq. (9) becomes of the form

$$n_\ell' = -\chi(R)\, f_\ell \qquad (14)$$

This system of coupled first order equations has been solved numerically using the Fourth-order Runge-kutta method[6] to generate the proton-waves.

C. THEORY OF PION ABSORPTION

According to the first order time independent perturbation theory, the differential crosssection for the (π^+,p) reaction is given by

$$\frac{d\sigma}{d\Omega} = \frac{M}{(2\pi)^2} E_o \frac{k}{q} \sum_f |\langle f|H|i\rangle|^2 \qquad (15)$$

where H is the Galilean invariant form of the non-relativistic reduction of the pseudo-scalar pseudo-vector interaction

$$H = \frac{f}{\mu} \sum_{i=1}^{4} \left[(1-\mu/2M)\, \vec{\sigma}.\vec{\nabla}_\pi \; \vec{\tau}.\vec{\phi} - \mu/M \; \vec{\tau}.\vec{\phi} \; \vec{\sigma}.\vec{\nabla}_N \right]_i \qquad (16)$$

Notations are similar to that employed in chapter 3 unless defined otherwise. The initial state $|i\rangle$ comprises of the positive pion and He^4 nucleus while the final state is made up of vacuum state of pionic field, the emitted proton and the residual nucleus He^3. The formalism employed is very similar to that of pion absorption by Lithium and Carbon. Hence the ingredients are sketched briefly.

C1 Pion distortion

The incident pion has a kinetic energy of 70 Mev and hence the following Klein-Gordon equation has been solved[7] to generate the pion waves.

Consequently

$$|f\rangle = \psi_p \, \psi_c(j-m') \qquad (24)$$

Scheme 2 :

In this scheme the proton-Helium 3 system has been studied through a variational approach as described in sec. B. The proton waves are generated by the solution of equation 9.

D. CALCULATIONS

The calculations have been done for the reaction $^4He\ (\pi^+,p)\ ^3He\ (g.s.)$. The incident pion energy is taken to be 70 Mev for reasons already stated (sec C chap. 3). All the requisite angular integrals have been solved exactly. Three kinds of pion-Nucleus optical potentials have been considered to account for the pion distortion viz : Standard Kisslinger form, Modified Kisslinger form and the Local Laplacian form. The potential parameters employed are the theoretical parameters listed in Table 3. The density function derived from our HF wavefunctions has been employed for the matter density. The coulomb potential has been calculated assuming the nucleus to be a spherically symmetric uniform charge distribution. The expansion coefficients $c^{\ell}_{\bar{n}n}$ used in the nuclear wavefunction are listed in Table 4. The proton optical well parameters for the square well potential are got from ref. 10.

Table 3

PION OPTICAL POTENTIAL PARAMETERS[a]

Nucleus	Re b_o	Im b_o	Re b_1	Im b_1	Remark
^{4}He	-0.70	0.40	6.30	1.20	Theoretical T_π = 66 Mev.

a) Auerbach et. al.[17]

Table 4

EXPANSION COEFFICIENTS C^{ℓ}_{nn}

Nucleus : Helium - 4

$os_{\frac{1}{2}}$ neutrons		
n = 1	n = 2	n = 3
0.9700	0.2152	0.1128

In the calculation of the crosssection employing scheme 2 for the final state proton distortion, the calculations have been done without considering pion distortion as otherwise the formalism becomes too cumbersome. The values of V_{ot} and V_{os} have been varied as free parameters to reproduce the correct order of magnitude consistent with the results of other method. The values of κ_t and κ_s are the same as in ref. 3.

E. RESULTS AND DISCUSSION

The calculations have been done taking into account pion distortion, nuclear correlations and proton distortion. The results are presented in Figs. 23 and 24. In Fig. 23 curve A represents the calculated results employing standard Kisslinger potential for pion distortion with the final state proton distortion accounted through high energy Glauber approximation. Curve B differs from curve A in that the pion distortion has been taken into account through Modified Kisslinger potential. The crosssection is slightly lower than that of curve A. The behaviour of this angular distribution of the crosssection is also similar to that of curve A. The calculated crosssection taking into account the pion distortion through the Local Laplacian potential is illustrated in Fig. 24 (let us say curve D for the discussion). The crosssection in this case is two orders lower than that of

FIG 23 : Differential crosssections for the reaction $^{4}He(\pi^{+},p)^{3}He$.

Curve A : Results obtained with Standard Kisslinger Potential.

Curve B : Results obtained with Modified Kisslinger Potential.

Case C : is the result of the calculation with protons distorted by a variational calculation and pion plane (scaled). Parameter values are V_{os} = 10 MeV V_{OT} = 20 MeV

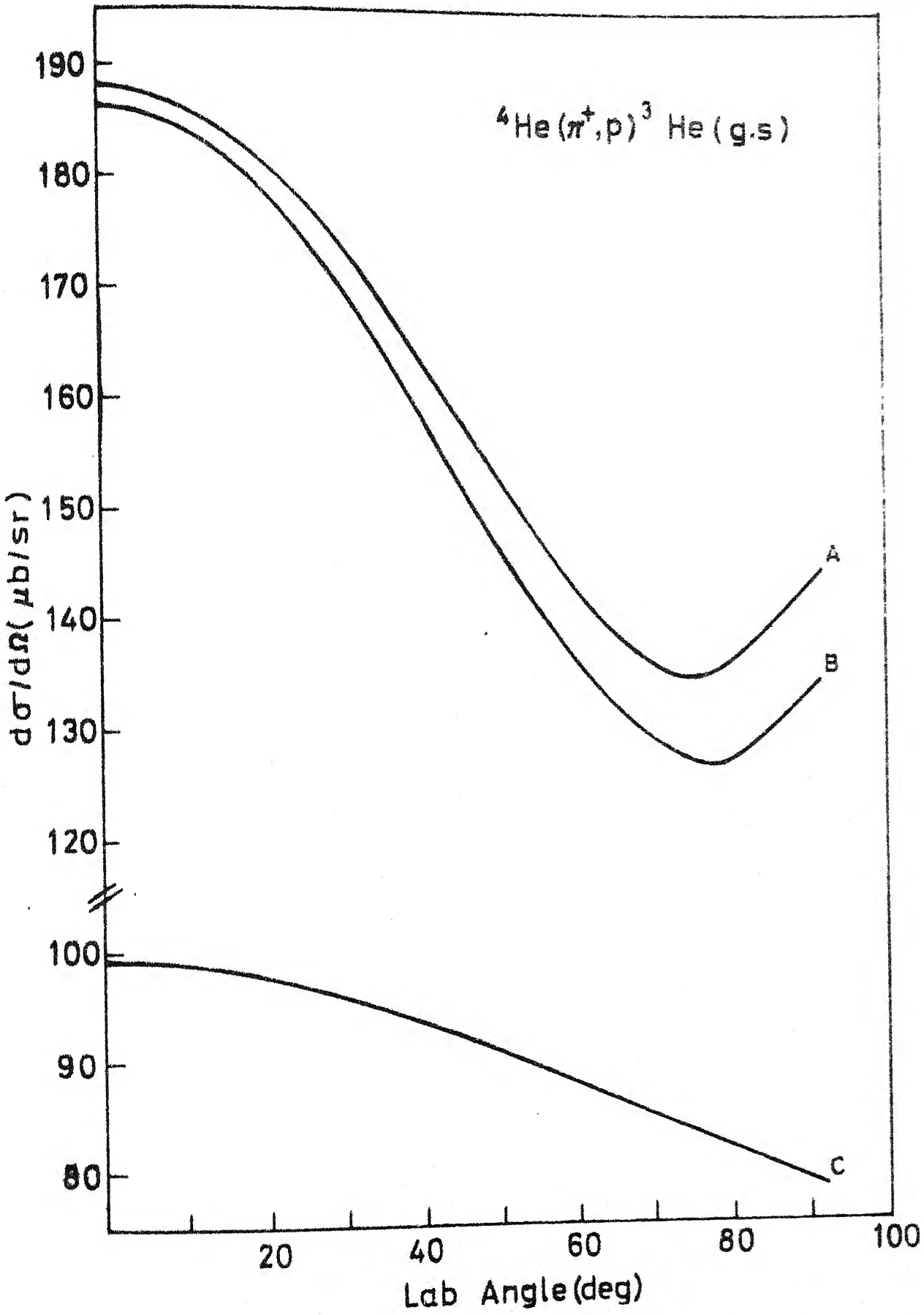
$^4He(\pi^+,p)^3$ He (g.s)
A
B
C
190
180
170
160
150
140
130
120
100
90
80
$d\sigma/d\Omega$ (μb/sr)
20
40
60
80
100
Lab Angle (deg)

FIG 24 : Differential crosssection for the reaction $^{4}He\ (\pi^{+},p)^{3}He$ using Local Laplacian form to distort pion waves (scaled).

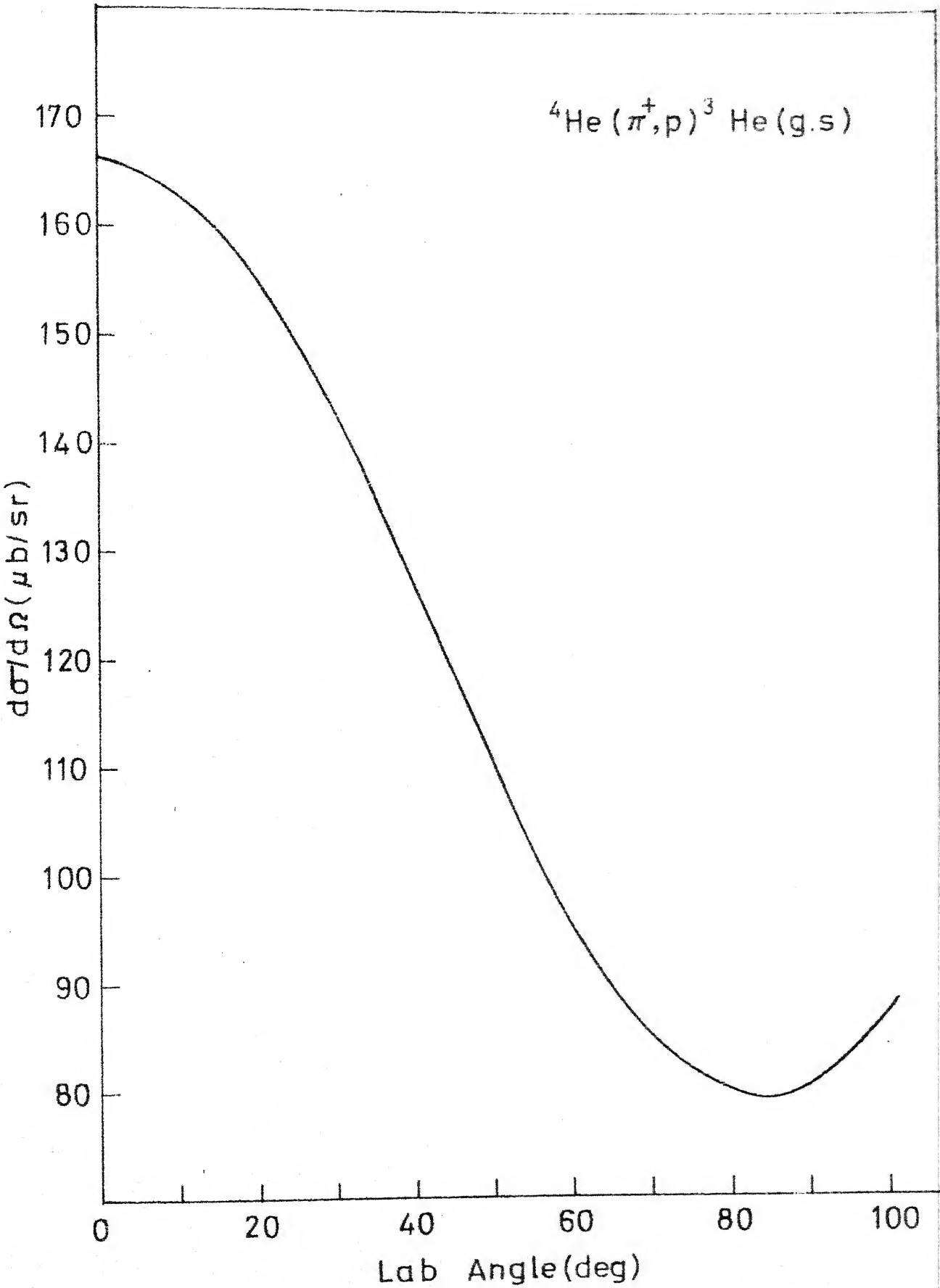
$^4He(\pi^+,p)^3He(g.s)$
170
160
150
140
130
120
110
100
90
80
$d\sigma/d\Omega(\mu b/sr)$
0
20
40
60
80
100
Lab Angle(deg)

FIG. 24

REFERENCES

1. I. Kakkar, Nuclear structure studies in Hartree-Fock Representation, Ph.D. Thesis, 1969, I.I.T. Kanpur (unpublished).

2. J. Wheeler, Phys. Rev. 52 (1937) 1107.

3. I. Reichstein, D.R. Thompson and Y.C. Tang, Phys. Rev. C3 (1971) 2139.

4. D.R. Thompson and Y.C. Tang, Nucl. Phys. A106 (1968) 591.

5. Karl. Wildermuth and Walter McCture in SPRINGER TRACTS IN MODERN PHYSICS ed. G. Hohler (Springer-Verlag Berlin N.Y. 1966) Vol. 41 p. 81.

6. Abramowitz. M. and I. Stegum in Handbook of Mathematics Functions (Dover Publication, NY.) formulas 25.5.10, page 896.

7. R.A. Eisenstein and G.A. Miller Comp. Phys. Comm. 8 (1974) 130.

8. R.J. Glauber in Lectures in Theoretical Physics ed.s. W.E. Britten and L.G. Dunham (Interscience N.Y. 1959) Vol. I p. 315.

9. D.U.L. Yu Ann. Phys. 38 (1966) 392.

10. G. Passatore Nucl. Phys. A110 (1968) 91, ibid A248 (1975) 509.

11. R.S. Kaushal and Y.R. Waghmare, Phys. Lett. B31 (1970) 637.

12. J. Letournex and J.M. Eisenberg, Nucl.Phys. 87 (1966) 331.

13. K. Gabathuler, J. Rohlin, J.J. Domingo, C.H.Q. Ingram, S. Rohlin and N.W. Tanner, Nucl. Phys. B40 (1972) 32.

14. B. Tatischeff et. al. Intern. Topical Conf. on Meson-Nuclear Physics, Carnegie-Mellon University (1976).

15. H. MuirHead in The Physics of Elementary Particles (Pergamon, London 1968) p. 27.

16. W.R. Gibbs and A.T. Hess, Phys. Lett B68 (1977) 205.

CHAPTER 5

CONCLUSION

CHAPTER 5

CONCLUSION

The present study includes all the factors like pion distortion, nuclear correlations and proton distortion. The analysis has indeed demonstrated the importance of these factors particularly nuclear correlations and pion distortion, in the presence of which all unnecessary sensitivities disappear. Further the calculation yields a higher value for the crosssection than the experimental result when one employes either Standard Kisslinger potential or Modified Kisslinger potential. Employing Local Laplacian potential, good agreement with experimental results have been achieved.

In this context, it has already been pointed out[1] that some of the partial waves generated by Standard Kisslinger potential exhibit peculiar behaviour at a radial distance of 1 fm. This is naturally disturbing because of the presence of dominant $\bar{\nabla}_{\pi}$ term in the interaction vertex coupled with the fact that crosssection depends upon the square of the matrix element. However earlier attempt to overcome this by Kroll-Kisslinger model has not been successful.

Further the pion reaction crosssections are sensitive to off-shell extrapolation one employes in the determination of optical potentials. The present analysis has amply demonstrated this. In addition, it emerges from our analysis that the Local Laplacian form is best suited, out of the three potentials studied, for such processes.

Another point to be noted, in the context of pion distortion, is the uncertainty in the value of Re b_o as has been demonstrated by the elastic scattering studies with pions. The small value of Re b_o stems from an almost exact cancellation between $\alpha=3$ phaseshifts and $\alpha=1$ phaseshifts (Eqn. 26, 27 Chap 2). Consequently any small error arising from impulse approximation, static approximation etc. are magnified in the final result.

In conclusion, it can be said that there is need for a correct off-shell extrapolation which can explain both elastic scattering data as well as pion reactions.

REFERENCES

1. W.B. Jones and M. Eisenberg, Nucl. Phys A154 (1970) 49.

APPENDIX

Hartree-Fock Density Distribution

The density of the particles inside the nucleus is

$$\rho_o(\vec{r}) = \int \sum_{\alpha=1}^{A} \left| \Psi(\vec{r}_1,\vec{r}_2,\ldots \vec{r}_{\alpha-1},\vec{r},\vec{r}_{\alpha+1}\ldots\vec{r}_A)\right|^2 d\vec{r}_1\, d\vec{r}_2\ldots d\vec{r}_{\alpha-1} d\vec{r}_{\alpha+1}\ldots d\vec{r}_A \qquad (A1)$$

where $\Psi(\vec{r}_1,\vec{r}_2\ldots\vec{r}_A)$ is taken to be fully antisymmetric product of an ortho-normal set of single particle wave-functions $\{\psi_\alpha\}$. Using this and integrating over A-1 coordinates, one obtains

$$\rho_o(\vec{r}) = \sum_{\alpha=1}^{A} \psi_\alpha^*(\vec{r})\, \psi_\alpha(\vec{r}) \qquad (A2)$$

But $\psi_\alpha(\vec{r})$ are single particle HF wavefunction related to Harmonic oscillator basis ϕ_μ through

$$\psi_\alpha(\vec{r}) = \sum_\mu C_\mu^\alpha\, \phi_\mu(\vec{r}) \qquad (A3)$$

where C's are expansion coefficients

Defining $$\rho_{\mu\mu'} = \sum_{\gamma=1}^{A} C_\mu^{\gamma *}\, C_{\mu'}^{\gamma} \qquad (A4)$$

eqn. A2 becomes

$$\rho_o(\vec{r}) = \frac{1}{A} \sum_{\mu\mu'} \rho_{\mu\mu'}\, \phi_\mu^*(\vec{r})\, \phi_{\mu'}(\vec{r})$$

where $\frac{1}{A}$ is added so that $\int \rho_o(\vec{r})\, d^3r = 1$.

$$\left.\frac{d\sigma}{d\Omega}\right|_{p\pi^+} = \frac{2J_A + 1}{2(2J_{A-1}+1)} \frac{q^2}{k^2} \left.\frac{d\sigma}{d\Omega}\right|_{\pi^+ p} \qquad (25)$$

where J_A is the total spin of Helium-4 system, J_{A-1} that of Helium 3, q and k are the momenta of pion and proton respectively. Employing the results of curve A in eqn. (25), the calculated differential crosssection for the reaction $^3He\ (p,\pi^+)^4He$ (g.s.) at $\theta = 0^o$ comes out to be 4 μb/sr. These are tabulated below for easier comparison. It should be remembered that the proton kinetic energy in this calculation is 150 Mev. The calculated crosssection compares favourably with the measured data.

Table 5

Reaction $^3He\ (p,\pi^+)^4He$

Kinetic energy of proton T_p	Differential crosssection $\frac{d\sigma}{d\Omega}$ for $\theta = 0^o$
600 Mev	18 ± 2 (a μb/sr
415 Mev	13 (b μb/sr
150 Mev	4 μb/sr our calculation

(a Data taken from ref. 13.

(b Data taken from ref. 14.

employing the standard Kisslinger form. The relative changes (Figs. 14-16) as the various effects are studied, are very similar to that of standard Kisslinger analysis. Hence an analysis here will only make it redundant.

3. LOCAL LAPLACIAN FORM

The features of the analysis when pion waves are generated by using the Local potential (eq. 3.12) are somewhat different from the earlier cases. Figs. 17 . studies the relative importance of different effects like pion distortion nuclear correlations and proton distortion. If all the effects are taken into account, curve A results. If the pion-nucleus optical potential is switched off then the crosssection falls by a factor of 7 unlike the earlier cases (curve B). On the other hand if the nuclear correlations are switched off, the reduction in the corsssection is by a factor of 6, thereby emphasising that nuclear correlations are as important. However if the emitted proton distortion is neglected then the crosssection is nearly doubled. Otherwise the behaviour with angle are very similar to the earlier cases.

The relative importance of the two terms in the interaction vertex are exhibited in Fig. 18. In view of the fact that the differential crosssection with pion distortion using Local potential is two orders of magnitude lower than the

Kisslinger form. Even though the near constancy of the crosssection for $\theta > 60^{\circ}$ is explained well, it does not explain the rise in the crosssection in the forward direction.

On the other hand, the calculated crosssection using the Local Laplacian potential reproduces the correct order of magnitude. This is compared with the experimental result in Fig. 22. The calculated values match well with the experimental crosssection for $\theta \geq 60^{\circ}$. The minima occuring around 70° gets shifted towards 50°. Further, in the forward direction, the peaking is better represented in comparison with the results of other two potentials, though not as pronounced as the experimental curve.

The above analysis of both carbon and Lithium indicate that when one considers the pion to be distorted by Local Laplacian potential, the results match well with experimental results than the case when the pion is distorted by either standard Kisslinger potential or Modified Kisslinger potential. Further the crosssection with the latter two potentials are nearly two orders of magnitude higher. The likely cause for this is as follows.

If one looks at the potential forms (eqs. 3.10-3.12) one finds that the nonlocal term $\bar{\nabla} \cdot \rho \bar{\nabla}$ which is present in the other two potentials is absent in the Local Laplacian potential. It has already been seen that the p-wave term is

37. G. Passatore, Nucl. Phys. A110 (1968) 91, ibid. A248 (1975) 509.

38. B.R. Wienke (Quoted in Ref. 3).

39. M.V. BarnHill, Nucl. Phys. A131 (1969) 106.

40. U.N.L. Mathur and Y.R. Waghmare (work in progress).

where $c_{\bar{n}n}^{\ell}$ are the mixing coefficients which induce the central correlations between the nucleons. ψ_c^{HF} represents the residual system.

C3 The outgoing proton wavefunction

The distortion of emitted proton in the field of residual nucleus has been included through two different ways, as already described.

Scheme 1

In this scheme, the proton-nucleus optical potential is assumed to be a complex square well, of strength

$$\begin{aligned} V &= -(U_o + iW_o) && r \leq R_o \\ &= 0 && r > R_o \end{aligned} \tag{21}$$

Since the proton energy is high, Glauber's high energy approximation[8] has been employed. In this approximation, the wavefunction of the outgoing proton is given by[9]

$$\psi_p = e^{i\vec{k}'\cdot\vec{r}}\, D\, \chi_{\frac{1}{2}\Lambda'} \tag{22}$$

where $D = \exp\left[-W_o M\bar{R}/k\right]$

with $\bar{R} = \langle (R_o^2 - r^2\sin^2\theta)^{1/2} \rangle = \frac{3R_o}{4}$, $\theta = (\hat{k},\hat{r})$ (23)

and $\vec{k}' = \vec{k}\left(1 + \frac{U_o M}{k^2} - i\frac{W_o M}{k^2}\right)$